Canadian Institute of
Guided Ground Transport
Queen's University
at Kingston, Ontario

prepared for the
Transportation Development Centre

by
S.T Lamson
C.A. Dixon

CIGGT Report No. 84-11
Transport Canada Report No. TP-6204E

CA2 ON
UQU 325
84
R11
c.2

CIGGT Project No. 313

CIGGT Report No. 84-11
TP-6204E

CIGGT TRACK RESEARCH PROGRAM

Interim Report
November 1983 - November 1984

Library and Information Centre
Centre de documentation (GSL)
RECEIVED — REÇU LE
JAN 18 1985
Government Publications Division
Transport Canada / Transports Canada

prepared for the

Transportation Development Centre

by

S.T. Lamson
C.A. Dixon

Canadian Institute of Guided Ground Transport
Queen's University at Kingston, Ontario
K7L 3N6

December 1984

This report resulted from research conducted through the Canadian Institute of Guided Ground Transport. The report represents the views of the authors and does not necessarily have the endorsement of the University or the other participating organizations.

REPORT DOCUMENTATION FORM

1. Transport Canada Report No.	2. TDC Project No.	3. Recipient's Catalogue No.
TP-6204E	6059	

4. Title and Subtitle	5. Report Date
CIGGT TRACK RESEARCH PROGRAM Interim Report - November 1983-November 1984	December 1984
	6. Performing Organization Report No. 84-11
7. Author(s) S.T. Lamson and C.A. Dixon	8. Transport Canada File No. D1465-401-2
9. Performing Organization Name and Address Canadian Institute of Guided Ground Transport (CIGGT) Queen's University Kingston, Ontario K7L 3N6	10. DSS File No. 11SD.T8200-3-3524
	11. DSS or Transport Canada Contract No. OSD 83-00120
12. Sponsoring Agency Name and Address Transportation Development Centre (TDC) Suite 2421, 1000 Sherbrooke Street West Montreal, Quebec H3A 2R3 CN Rail, P.O. Box 8100 Montreal, Quebec H3C 3N4	13. Type of Report and Period Covered Interim - 11/83-11/84
	14. Sponsoring Agency Code TDC 6059
15. Supplementary Notes	16. TDC Project Officer W. Rowan

17. Abstract

A comprehensive long-term program aimed at developing practical and cost-effective techniques to reduce track geometry and component deterioration and a systematic approach to track maintenance planning to improve cost and time efficiency was initiated in November 1983. The main thrust of the first year's research was to formulate the relationship between traffic loading and track response based on current knowledge of vehicle dynamics and track behaviour. Computer programs thus produced are useful tools for analysis of track maintenance requirements and costs. Details of computer programs for track characterization, vehicle dynamic simulation, rail joint settlement prediction, tie life prediction and turn-out maintenance estimation are presented.

18. Key Words	19. Distribution Statement
Track dynamics, Vehicle dynamics, Tie, Rail, Plastic deformation, Settlement, Wheel forces, Simulation, Track system, Track geometry, Impact	Restricted

20. Security Classification (of this report)	21. Security Classification (of this page)	22. No. of Pages	23. Price
unclassified	unclassified	6 + append.	

FORMULE DE DOCUMENTATION POUR RAPPORT

1. N° du rapport Transports Canada	2. N° de l'étude — CDT	3. N° de catalogue du destinataire
TP-6204E	6059	

4. Titre et sous-titre	5. Date du rapport
CIGGT TRACK RESEARCH PROGRAM Interim Report - November 1983-November 1984	Décembre 1984
	6. N° du rapport de l'organisme exécutant 84-11
7. Auteur(s) S.T. Lamson and C.A. Dixon	8. N° de dossier Transports Canada D1465-401-2
9. Nom et adresse de l'organisme exécutant Canadian Institute of Guided Ground Transport (CIGGT) Queen's University Kingston, Ontario K7L 3N6	10. N° de dossier — ASC 11SD.T8200-3-3524
	11. N° de contrat — ASC ou Transports Canada OSD.83-00120
12. Nom et adresse de l'organisme parrain Centre de développement des transports (CDT) 1000 o., rue Sherbrooke, Suite 2421 Montréal, Québec H3A 2R3 Chemins de fer Nationaux du Canada CP 8100, Montréal, Québec H3C 3N4	13. Genre de rapport et période visée Provisoire--11/83-11/84
	14. Code de l'organisme parrain TDC 6059
15. Remarques additionnelles	16. Agent de projet — CDT W.G. Rowan

17 Resume

En novembre 1983, un programme de longue haleine a été lancé dans le but d'étudier des techniques fiables et économiques visant à atténuer la dégradation de la géométrie des voies ferrées et de ses éléments constitutifs et, en même temps, à dégager une méthode de planification systématique de la maintenance débouchant sur un accroissement de l'efficacité des interventions et une diminution des coûts correspondants. La première année de ce programme de recherche a été consacrée à la recherche du rapport qui pourrait exister entre les charges imposées aux voies et les réactions de celles-ci, mettant à profit les connaissances acquises en matière d'interaction dynamique roue-rail. Les programmes de calcul informatisés qui ont pu être formulés jusqu'ici se sont révélés très utiles pour définir les critères de maintenabilité des voies et pour estimer les coûts. Le rapport présente en détail les travaux effectués pour caractériser les voies, simuler le comportement dynamique du matériel roulant, calculer le tassement des rails aux joints et prédire la durée de vie des traverses ainsi que la périodicité de l'entretien des appareils de voie.

18. Mots-clés	19. Diffusion
Dynamique. Voies ferrées. Matériel roulant. Traverses. Rails. Déformation plastique. Tassement. Sollicitation. Simulation. Voie ferrée. Géométrie de voie. Chocs.	Diffusion restreinte

20. Classification de sécurité (de ce rapport)	21. Classification de sécurité (de cette page)	22. Nombre de pages	23. Prix
non classifié	non classifiée	6 + append.	

CDT TDC 79-005

TABLE OF CONTENTS

1. INTRODUCTION 1

2. WORK ACCOMPLISHED 4
   - 2.1 Track Characterization Technique 4
   - 2.2 Wheel Load Characterization Technique 5
   - 2.3 Track Dynamic Model 6
   - 2.4 Rail Joint Maintenance Model 6
   - 2.5 Turn-Out Maintenance Model 6
   - 2.6 Tie Life Model 6

Appendix A: TRACK CHARACTERIZATION TECHNIQUE

Appendix B: WHEEL LOADING CHARACTERIZATION TECHNIQUE

Appendix C: TRACK RESPONSE MODEL

Appendix D: RAIL JOINT MAINTENANCE MODEL

Appendix E: TURN-OUT MAINTENANCE MODEL

Appendix F: TIE LIFE MODEL

1. INTRODUCTION

Canadian railways have experienced a rapid increase in traffic growth during the last two decades. This increase has been accommodated by a large increase in axle loads, train speeds and train lengths, as well as some modest track capacity expansionary construction. On some of the most heavily loaded lines, the railways have made significant investments in track upgrading to offset accelerated wear rates.

It is expected that traffic growth will continue. This creates demand for further increases in axle loads, train lengths and traffic density, since track capacity expansionary construction is very costly. The Australian iron ore railways recently experimented with a train length of 230 cars, an axle load of 35 tonnes and a speed of 85 km/h. Rail wear and track geometry deterioration are likely to increase, creating a greater requirement for track maintenance, precisely when less track occupancy time for maintenance can be made available.

To make an effective contribution to the improvement of productivity in Canadian railways, the Transportation Development Centre of Transport Canada has sponsored a government/industry cooperative track research program. This program has a three-year horizon, and aims at developing (a) practical and cost-effective techniques to reduce track geometry and component deterioration, and (b) a systematic approach to track maintenance planning to improve cost and time efficiency. At the same time, the program also aims to foster basic track support and structure basic research to ensure the researcher's long-term ability to support track maintenance innovations.

The main thrust of the first year's research, which commenced in November 1983, was to formulate the relationship between traffic loading and track response based on current knowledge of vehicle dynamics and track behaviour. The work was oriented toward producing useful tools for the analysis of track maintenance requirements and costs.

Figure 1 is a schematic diagram of the track system. It describes the main interactive processes which link the vehicle dynamic force inputs experienced by the track to the deterioration of track components and geometry. As shown, a vehicle of a given design, running over a

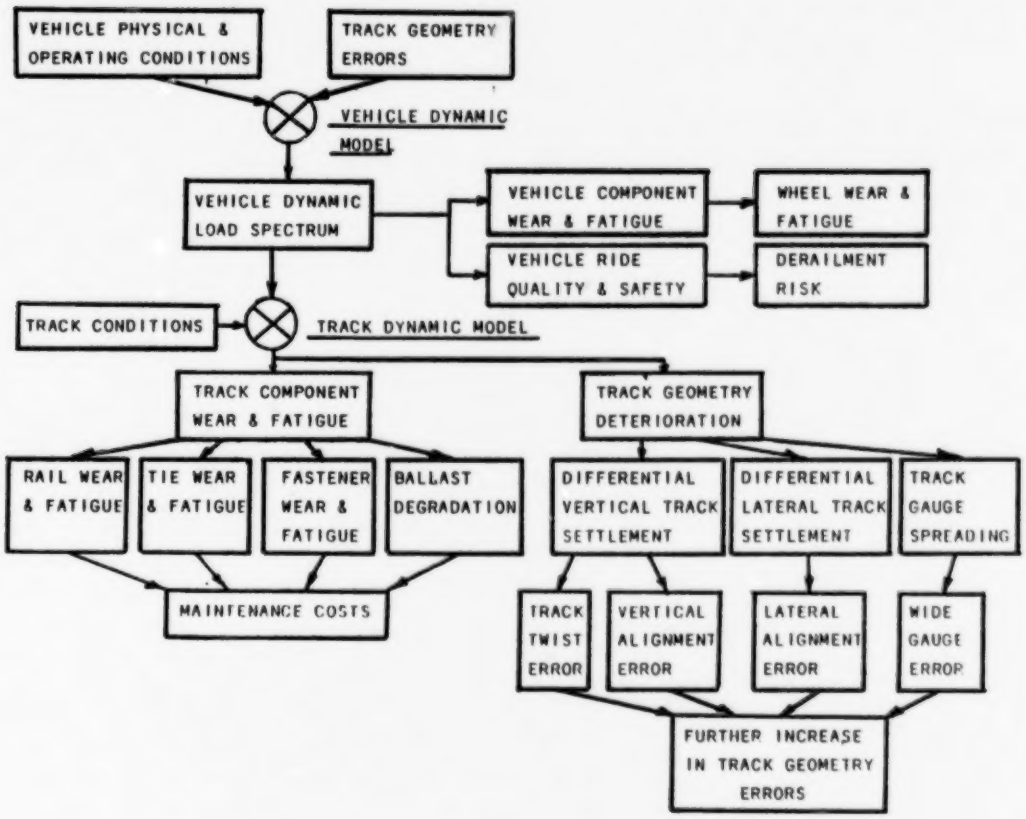

Figure 1 Track system

track section of a given standard, at a given speed, will create a spectrum of track forces.

These forces are transmitted into the track, causing wear and fatigue of track components and deterioration of track geometry. The distribution of these forces depends on track design and the condition of the track components. Repair and replacement costs are incurred due to component wear and fatigue. Deterioration of track geometry increases track errors and leads to larger dynamic wheel loads as subsequent trains pass. This cycle continues until track components and geometry are reconditioned. Thus, vehicle performance and track response are inter-related, and the track deterioration process is generally self-accelerating.

To understand and quantify the behaviour and interaction of such systems, the following work must be carried out:

(a) **Determination of track loading.** In North America, dynamic track loadings have traditionally been derived from static wheel loads and track curvatures using empirical formulae. Accuracy is limited, since these formulae are typically based on outdated experiments. The development of rolling stock in the last few decades has resulted in a variety of vehicle designs with distinctively different dynamic performances on track. Recent advances in computer technology have made it possible to improve these loading estimates greatly through the use of computer models which can conveniently simulate the performance of several types of vehicles over various track conditions. These computer models provide more detailed information such as dynamic wheel loads in vertical, lateral and longitudinal directions. These data are essential for evaluating track loading resulting from various vehicle designs, vehicle operations and track standards.

(b) **Determination of track response.** For any given set of dynamic wheel forces from given traffic, there is a corresponding set of forces on ties and ballast. This load distribution varies with track configuration and track component conditions. One common technique for estimating load distribution is based on the theory of beam (rail) on elastic foundation (ties and ballast). Once the load distribution is known, Boussinesq's equation can be applied to estimate the stresses in ballast, subballast and subgrade.

(c) **Estimation of track component deterioration rate.** Steps (a) and (b) produce data describing the loading (i.e. forces/stresses) on each track component. Based on this data, estimates of wear and fatigue rates of track components such as rails and ties can be made. These will indicate the level of track maintenance effort which a given track design would require in the long term under a specified traffic level. The CIGGT Rail Wear Cost Model is an analytical tool for this purpose.[1]

---

1 E.R. McIlveen, A.M. Birk, J.D. Young, R. Glaser. CIGGT Rail Wear Cost Model: User's Manual. CIGGT Report 81-19, April 1982.

(d) **Estimation of track geometry deterioration rate.** Since conventional track design is not rigid, the continued application of wheel loads leads to track settlement. Further, because wheel forces generally vary along the track, the settlement is not uniform. This leads to further increases in track geometry errors and, in turn, to further increases in wheel forces. Research work in the area of track settlement has resulted in some understanding of track settlement behaviour. This can be used to constructed a preliminary model of track differential settlement for use in analyzing track geometry deterioration problems.

2. WORK ACCOMPLISHED

2.1 Track Characterization Technique

A set of computer programs has been developed to convert the track geometry error data, such as those gathered by CP and CN track recording cars, into computer files for vehicle/track dynamic interaction analysis. These programs include:

(a) a digitization program which converts the track geometry error data from brush charts into a set of (x,y) data points

(b) a Fourier fit program which performs a Fourier transformation of the (x,y) data points; the transformed data provide wheel inputs in terms of displacement, velocity and acceleration for a given vehicle speed

(c) a track index program which calculates the standard deviation, frequency and CN-type quality index for surface and cross-level track errors.

These programs enable the characterization of any sample track section and the conversion of the track geometry data into the right format for vehicle dynamic simulation studies.

These programs are detailed in Appendix A.

2.2 Wheel Load Characterization Technique

A set of computer models has been developed for the simulation of a railway vehicle dynamic response over a sample of actual track. These include:

(a) a vertical dynamic vehicle model which simulates the dynamic response of a four-axle railway vehicle running at a given speed over a track with given surface and cross-level errors. Simulation outputs include the dynamic vertical wheel/rail forces which are essential for the analysis of traffic-induced track damage. Model parameters can be appropriately chosen to represent various types of four-axle vehicles such as 100-ton cars, locomotives or passenger coaches.

(b) a steady-state truck curving model which simulates the steady-state curving behaviour of a three-piece truck on a track with a given degree of curvature and rail profile. Simulation outputs include the steady-state wheel forces and angle of attack at each axle. These data are essential for the estimation of rail wear and tie life under a given type of traffic.

(c) a lateral dynamic vehicle model which simulates the dynamic response of a four-axle railway vehicle to track alignment error. Simulation outputs include the dynamic variation of the lateral wheel/rail forces. These data can be combined with the steady-state lateral wheel forces (simulated with the truck curving model) to obtain an estimate of the dynamic wheel forces in the lateral direction.

These models permit the estimation of the vertical and lateral dynamic wheel forces produced by a given vehicle running at a given speed over a track with a given geometry error level. These are the necessary inputs for analyzing traffic-induced track component and geometry deterioration problems.

Details of these models are given in Appendix B.

2.3 Track Response Model

The track response model predicts the distribution of dynamic wheel loads from various rail vehicles onto the track structure and support components. The stresses and deformations predicted by this model are key to the analysis of effects of traffic on the deterioration of track components and gometry. A detailed report on this model is given in Appendix C.

2.4 Rail Joint Maintenance Model

This track settlement model predicts the dynamic forces exerted by various traffic categories on dipped joint geometries. Associated stresses in ballast and subgrade are calculated and cumulative strain levels determined. The strain levels are used to predict ballast settlement. As track geometries deteriorate, wheel impact forces increase, initiating further settlement. This model is described in Appendix D.

2.5 Turn-Out Maintenance Model

This model estimates the proportion of damage to turn-outs attributable to different traffic categories on a given line. The calculations are based on the plastic deformation of frogs and switches due to impact wheel loads. The British Rail formula for impact load (P_2) is used to calculate impact wheel loads at frog noses and switch blades. Plastic deformation is calculated according to the most current theory on shakedown limit. A detailed report of the model is given in Appendix E.

2.6 Tie Life Model

This model predicts the required rate of tie renewal for a given track under given traffic. The track is characterized by its geometry and roughness. The traffic is characterized by axle load, speeds and density. The model also gives estimates of the renewal requirements broken down into per-track and per-traffic categories. It is, therefore, a useful tool for track maintenance and resource allocation planning. Details of this model are given in Appendix F.

APPENDIX A

TRACK CHARACTERIZATION TECHNIQUE

A.1 DIGITIZATION PROGRAM

Program DIGIT was written to digitize track geometry error data such as those shown in Figure A.1 to produce suitable input data for computer analysis of track characteristics. The program is written in FORTRAN and operates in an interactive mode. A Hewlett-Packard plotter/digitizer is used to register the track coordinate readings. These readings are stored on files by an IBM PC. Several quarter-mile sections of CN track have been digitized to create a computer file of typical CN track error conditions.

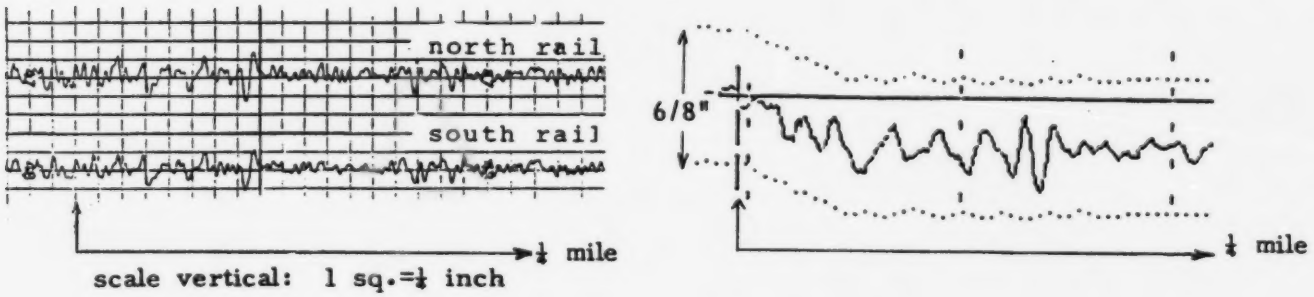

VERTICAL SURFACE ERROR LATERAL SURFACE ERROR

Figure A.1 Vertical and lateral rail profiles as per brush chart recordings

A.2 FOURIER FIT PROGRAM

This program performs a Fourier transformation on the (x,y) coordinates of track geometry errors created from the digitization routine. A file of Fourier coefficients is created representing the amplitudes of all wavelengths in the Fourier strings. For a reproduction accuracy of track geometry error wavelengths of 2 m and greater, 200 Fourier coefficients are used.

From these coefficients, the characterization of the track in terms of vertical displacements (x,y), velocities (dy/dx) and accelerations (d^2y/dx^2) are derived. These data are used as track input to each wheel in a vehicle dynamic simulation study.

A.3 TRACK INDEX PROGRAM

This program calculates the following characteristics for each 30 m section of track geometry errors:

- standard deviation (amplitude indicator)
- frequency index (an indicator of the predominant wave length)
- CN track quality index (an indicator of the product of frequency and amplitude)

Sample output from this program is shown in Figures A.2 through A.5.

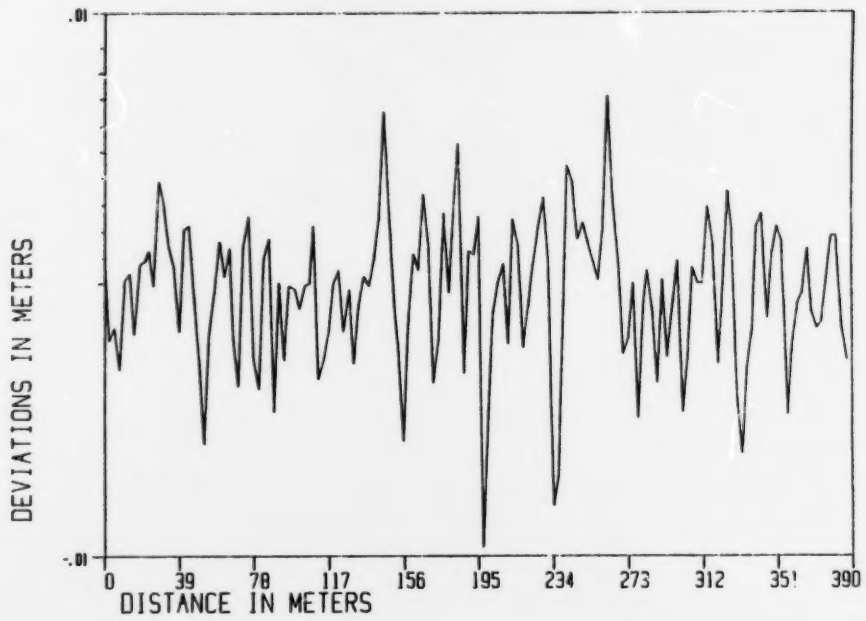

Figure A.2 Digitized surface errors

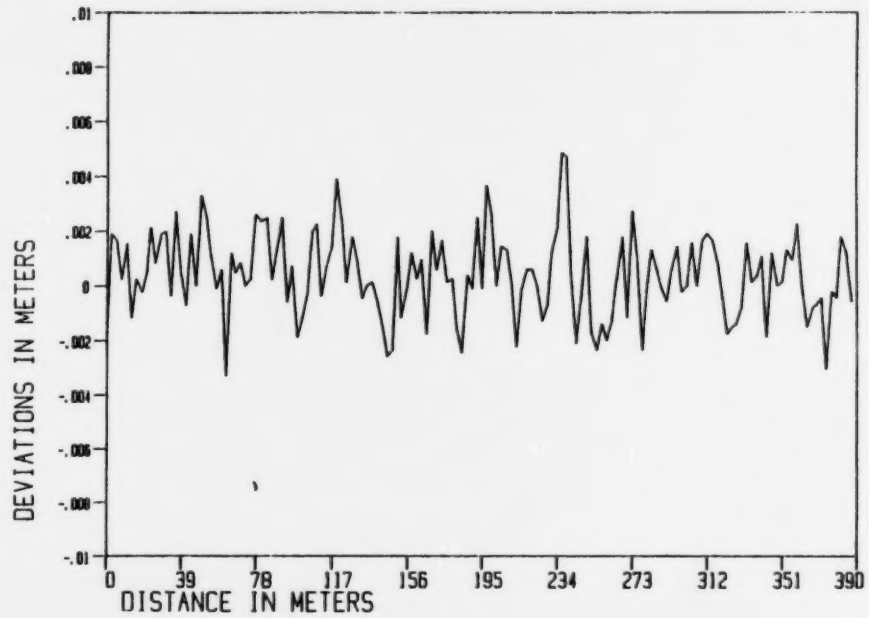

Figure A.3 Digitized cross-level errors

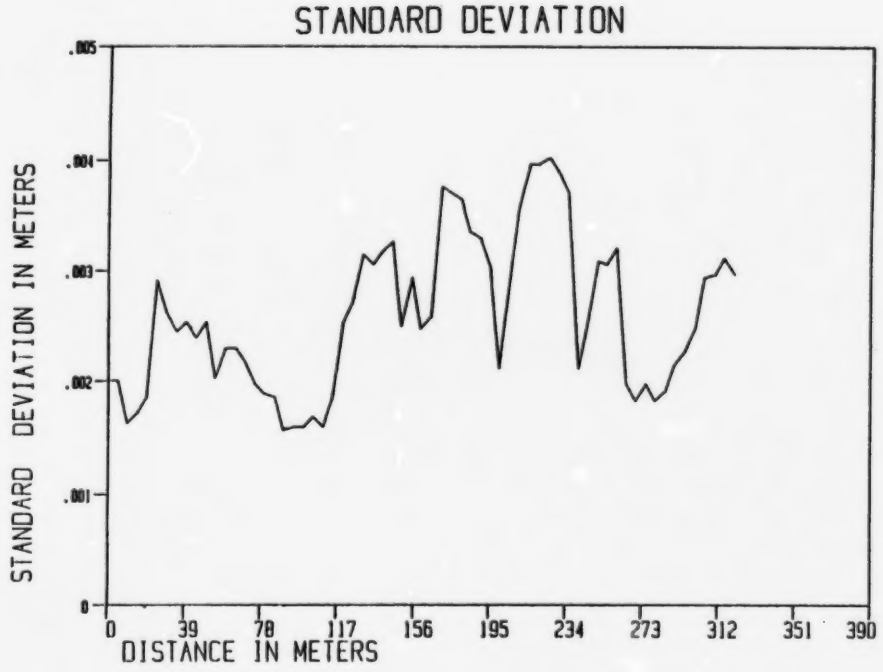

Figure A.4 Standard deviation of surface error

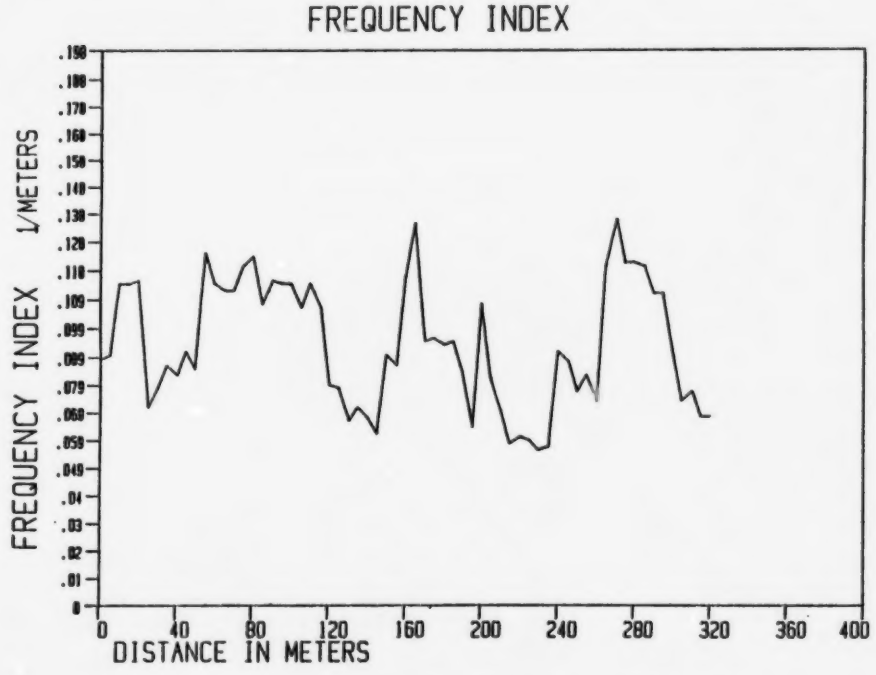

Figure A.5 Frequency index of surface error

APPENDIX B

WHEEL LOADING CHARACTERIZATION TECHNIQUE

B.1 VERTICAL VEHICLE DYNAMICS MODEL

B.1.1 Description

This model simulates the dynamic response of a four-axle vehicle to random surface irregularities. Of prime interest are the dynamic wheel/rail forces and carbody acceleration. Additional data such as dynamic forces between individual vehicle components and their velocities and accelerations may be generated as required.

A diagram of the model is shown in Figure B.1.

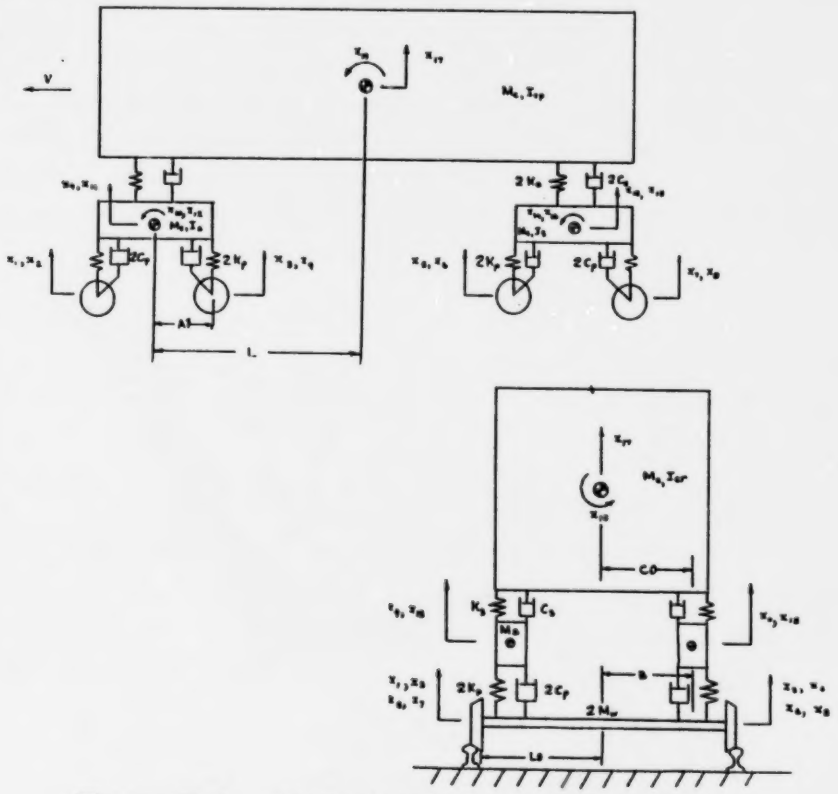

Figure B.1 Vertical vehicle dynamics model

The model is a simplified representation of any four-axle vehicle such as a 100-ton car, a four-axle locomotive, etc. It has 19 degrees of freedom:

(a)	wheel heave (8)	$x_1, \ldots x_8$
(b)	sideframe heave (4)	$x_9, x_{11}, x_{13}, x_{15}$
(c)	sideframe pitch (4)	$x_{10}, x_{12}, x_{14}, x_{16}$
(d)	carbody heave	x_{17}
(e)	carbody pitch	x_{19}
(f)	carbody roll	x_{18}

Each wheelset is connected to the sideframes with a primary spring and damper. Each sideframe is connected to the carbody with a secondary spring and damper. If the model is to be applied to another vehicle for which any of these springs or dampers do not exist, their value can be appropriately adjusted.

This model considers three basic assumptions. First, all mass components (namely sideframes, carbody, wheelsets) are assumed to be rigid. Second, all wheelsets are assumed to always be in contact with the rails. Third, all springs and dampers behave linearly.

B.1.2 Vehicle Input Data

A complete list of vehicle data required for vertical dynamic response simulation is given below. The masses, springs and dampers are labeled in Figure B.1.

A_1 = half axle spacing
B = half distance between primary suspension elements
C_o = half distance between secondary suspension elements
L_o = half distance between wheels
L = distance carbody centre-of-gravity to secondary suspension
M_{ax} = mass of wheel and half-axle
M_{sf} = mass of sideframe
M_{bod} = mass of carbody

I_{sf} = sideframe inertia
I_{rot} = carbody rotational inertia
I_{pt} = carbody pitch inertia
K_1, K_2 = primary, secondary spring stiffness
C_1, C_2 = primary, secondary damping coefficients

These input data are stored in computer files which are read by the main program during the simulation runs. Dynamic simulations may be made for any four-axle vehicle operating at any speed by creating a data file with the corresponding parameters. Heavy and light freight cars, passenger coaches and four-axle locomotives can all be represented by this model. A sample data set representing a 100-ton hopper car is shown below.

A_1 = 0.9 m
B = 1.003 m
C_o = 1.003 m
L_o = 0.7176 m
L = 5.5 m
M_{ax} = 7.1×10^2 kg
M_{sf} = 7.3×10^2 kg
M_{bod} = 4.5×10^2 kg

I_{sf} = 1.1×10^5 kg/m^2
I_{rot} = 3.6×10^4 kg/m^2
I_{pt} = 1.8×10^6 kg/m^2
K_1 = 2.827×10^7 N/m
K_2 = 3.88×10^6 N/m
C_1 = 6.2×10^4 Ns/m
C_2 = 1.11×10^5 Ns/m

B.1.3 Track Input Data

This model can simulate the vertical dynamics of vehicles over idealized track and actual track. For the latter case, the digitized track geometry data (e.g. surface roughness and cross-level error) must be used as track input data).

Recent applications of this model to CN traffic employed actual rail surface errors which were digitized from CN track geometry brush chart recordings.

B.1.4 Output

The dynamic vertical wheel/rail forces and carbody accelerations are the main outputs. Other output options include:

- mean and standard deviation of vehicle forces
- carbody displacement and velocities
- sideframe and wheel acceleration velocities
- energy dissipation in the suspension system (as a component of train resistance).

The vertical dynamic forces calculated with this model serve as force input to other track maintenance models developed concurrently in this research program.

B.1.5 Sample Vertical Dynamic Simulation

Figure B.2 shows the dynamic wheel/rail forces exerted by a 100-ton car (parameters shown previously) running at 60 mph along a 40 m track length. Figure B.3 shows an example output option on the energy dissipation.

B.2 STEADY-STATE TRUCK CURVING MODEL

This model simulates the steady-state curving behaviour of a three-piece truck under a railway vehicle. A schematic diagram of the model is shown in Figure B.4. Leading and trailing wheel sets are assumed to be parallel. This leaves the model with three degrees of freedom, namely:

- wheelset lateral displacement
- wheelset angle of attack
- truck frame lozenging angle.

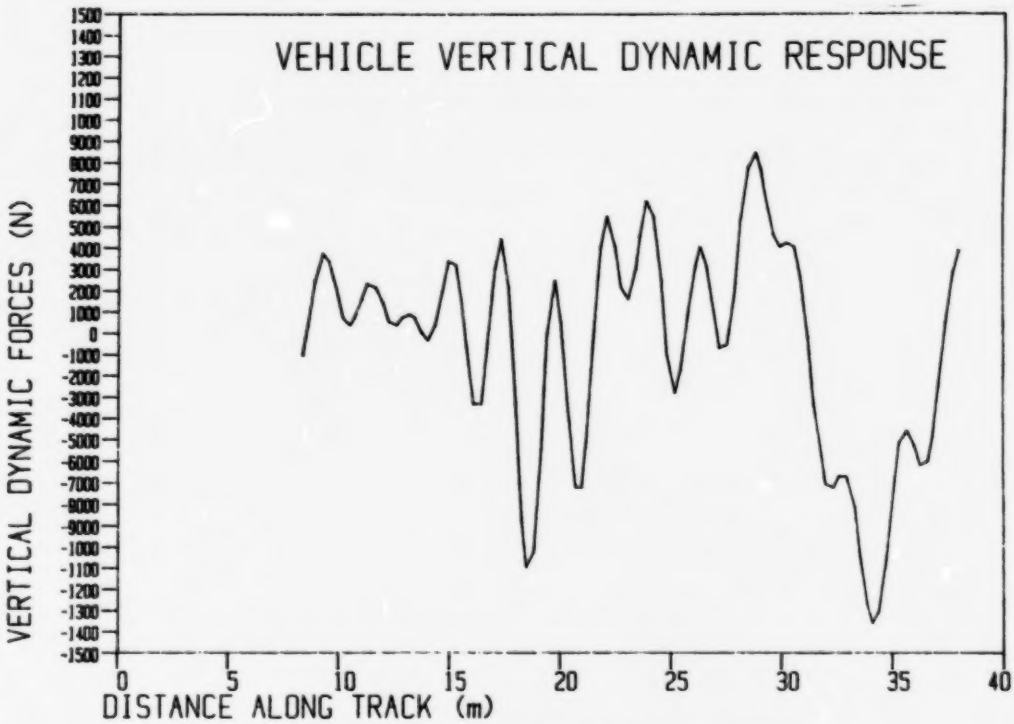

Figure B.2 Vertical vehicle dynamic response

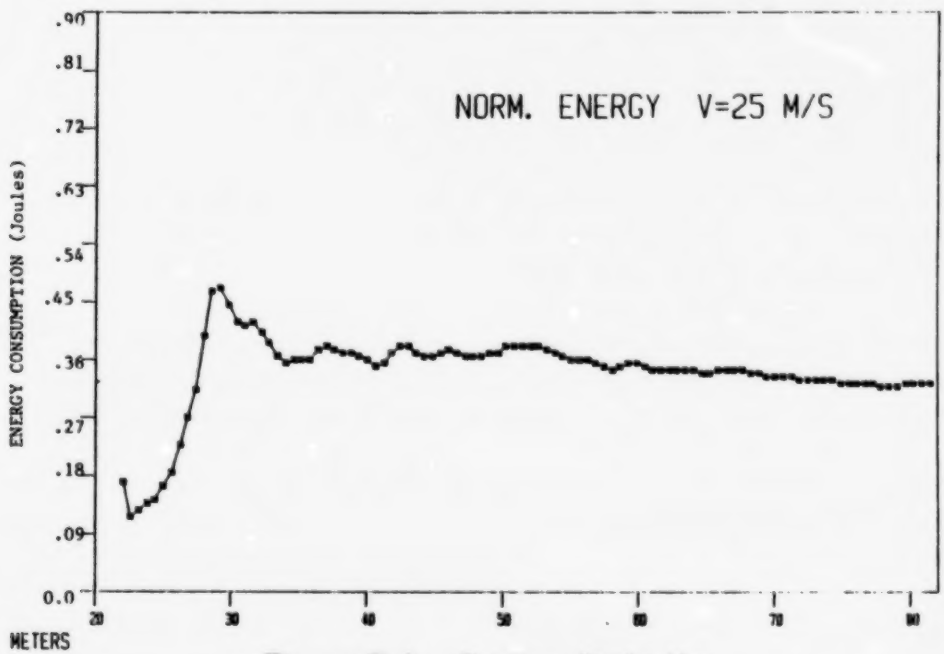

Figure B.3 Energy dissipation

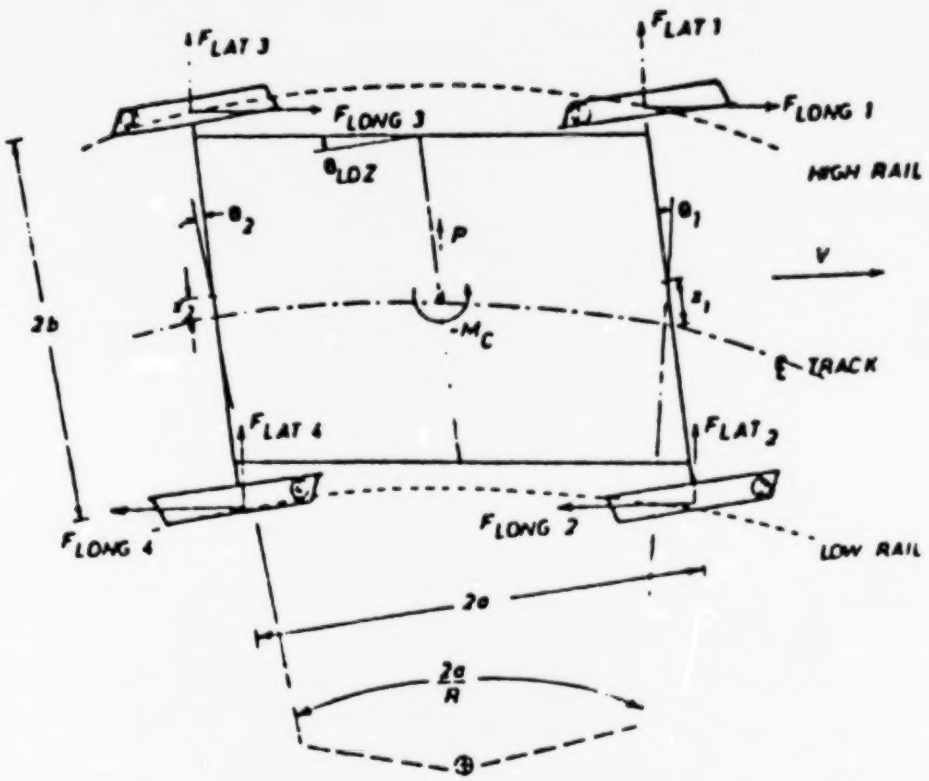

Figure B.4 Schematic diagram of truck curving model

Two common truck curving modes, non-flanging (in shallow curves) and flanging (in sharp curves), can be simulated, making the model useful for a wide range of curve degrees.

Non-linear interaction characteristics of in-service wheel and rail profiles are incorporated in the simulation, rendering the model suitable for the evaluation of the effect of modifying wheel and rail profiles.

Non-linear creep coefficient and different levels of rail lubrication can be simulated, making the model suitable for the evaluation of the effect of track lubrication.

The model is written in FORTRAN and operates in an interactive mode. A set of default values for track, vehicle and operational parameters

are built in for model inputs. Any of these can be modified by the user. A complete list of the model inputs and the default values are given below.

Input			Default Values for Truck on 3° Curve for Two-Point Contact Mode
WBASE	=	wheelbase (m)	1.83 m
BCD	=	truck centre distance (m)	5.20 m
H	=	COG/rail head vertical distance (m)	2.00 m
CLOZ	=	lozenging stiffness (kNm/rad)	36,000 kNm/rad
MC	=	rotational resistance (kNm)	0.0 kNm
R	=	curve radius (m)	582.0 m
GAUGE	=	track gauge (m)	1.44 m
SUPEL	=	superelevation (m)	0.064 m
VKPH	=	vehicle velocity (kph)	57.50 km/m
GWT	=	vehicle gross weight (tonne)	125.0 tonnes
MU	=	flange friction factor	0.30
MODE	=	one- or two-point contact	2.0
C1LON C2LON C3LON C4LAT C5LAT C6LAT	=	creep co-efficient equation constants	

Model outputs cover data on track position (lozenging angle), lateral displacement, truck configuration (lozenging angle), wheel/rail interaction forces (creep forces, flanging force, vertical wheel load transfer, etc.) and wheel/rail creepages. Tread and flange wear indices are also provided for wheel and rail wear evaluation. A complete output printout is shown in Figure B.5.

```
      CURVE MODEL          RUN NUMBER     3                  02:23:46

                           2POINT CONTACT MODE

LEADING WHEELSET           AAR20.DAT                 AAR 1 IN 20 CONE WHEEL
TRAILING WHEELSET          AAR20.DAT                 AAR 1 IN 20 CONE WHEEL

VEHICLE                    TRACK                     OPERATION

WBASE       1.830M         R          582.0M         VKPH       57.50KM/H
BCD         5.200M         GAUGE     1.4400M
                                                     GWT       125.00TONNE
H           2.000M         SUPEL     0.06400M       MU        0.30000
PHID       39.989DEG.      FRC1      0.01100M
CLOZ      36000.0KNM/RAD   FRC2     -0.01100M       CENTRIFUGAL FORCE
MC          0.000KNM       FRC3      0.01100M
                           FRC4     -0.01100M       P          -0.156KN

CREEP COEFF EQN CONSTS.    ITERATION CONTROLS        EQUILIB. EQN. ERRORS

C1LON       138.0          DWT         4.000KN       ERLAT    -0.03963KN
C2LON         0.0          DLXX1     0.00050M        ERROT    -0.06978KNM
C3LON         0.1          DTXX2     0.00100M        ERLOZ    -0.06978KNM
C4LAT       138.0          EQERR     0.10000         ERTQL     0.09760KNM
C5LAT     70000.0          EPS     1.000E-06         ERTQT    -0.01407KNM
C6LAT     -1570.0          INTRM          50

WHEEL LOADS                TRUCK CONFIGURATION       CONTACT POINT RADII

W1        153.386KN        X1         0.01100M       R1        0.48550M
WT         81.511KN        X2         0.00752M       RXFC      0.49550M
W2        153.170KN        THTA1   2.812E-03RAD      R2        0.48450M
W3        153.386KN        THTA2  -3.322E-04RAD      R3        0.48533M
W4        153.170KN        THLOZ  -6.641E-04RAD      R4        0.48467M

LONG. CREEPAGES            LONG. CREEP CO-EFF        LAT. CREEP CO-EFF

CRL1   -2.401E-03          CL1         -0.201 MU     CT1         0.218MU
CRL2    1.984E-03          CL2          0.180MU      CT2         0.218MU
CRL3   -5.654E-04          CL3         -0.069MU      CT3        -0.043MU
CRL4   -5.654E-04          CL4         -0.069MU      CT4        -0.043MU

GRAVITATIONAL FORCES       LONG. CREEP FORCES        LAT. CREEP FORCES

FG1         4.076KN        FL1        -16.350KN      FT1        17.746KN
FG2         7.658KN        FL2         27.504KN      FT2        33.347KN
FG3         7.669KN        FL3        -10.538KN      FT3        -6.521KN
FG4         7.658KN        FL4        -10.523KN      FT4        -6.512KN

FLANGE FORCES              RESULTANT LONG. FORCES    RESULTANT LAT. FORCES

RF        143.701KN        FLON1      26.761KN       FLAT1     -27.845KN
RFL        43.110KN        FLON2      27.504KN       FLAT2      41.006KN
RFT        41.516KN        FLON3     -10.538KN       FLAT3     -14.191KN
                           FLON4     -10.523KN       FLAT4       1.146KN

WEAR INDICES               ITERATION COUNTERS

                                                     ITXWT         28
WTRD      0.25374          ITAVL         23          I1XX1          0
WFLNG     0.08795          ITAVT          1          ITXX2         13
```

Figure B.5 Sample output, truck curving model

B.3 LATERAL DYNAMIC VEHICLE MODEL

This model simulates the response of a four-axle railway vehicle to random alignment errors in curved track. This reponse includes the dynamic variation of the lateral wheel forces about its mean value. Figure B.6 shows an example of the dynamic lateral force at the leading wheel of a railway vehicle during curving. The mean (steady-state) value can be estimated by the truck curving model described in Section B.2. The dynamic variation can be estimated using this model.

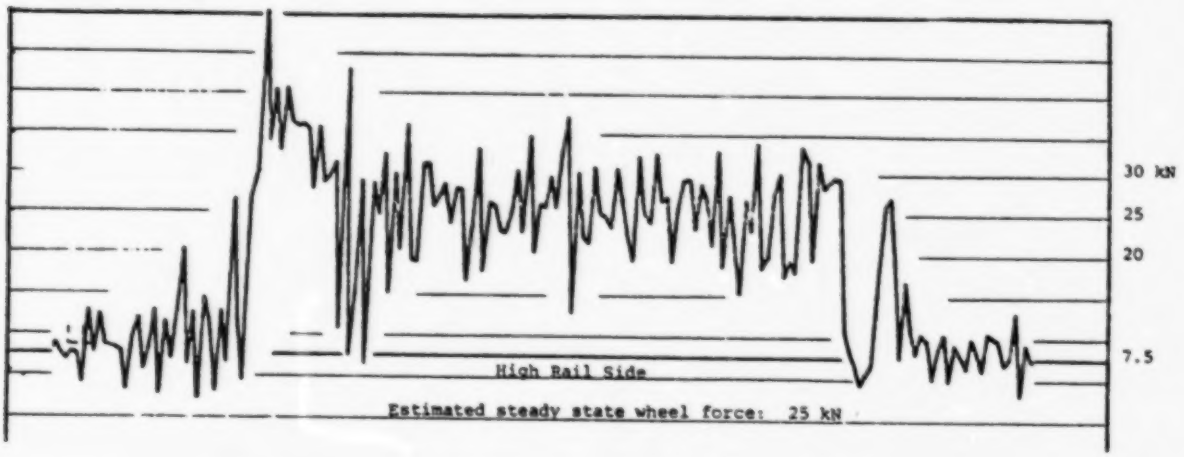

Figure B.6 Example of dynamic lateral force

This model assumes that the vehicle travels in a flanging mode, i.e. wheel flanges are in constant contact with the high (outer) rail. This is often the case in sharp curves. In shallow curves usually only the leading wheel of each truck is in flange contact. In this case the prediction will be conservative.

A schematic diagram of the model is shown in Figure B.7. It has 12 degrees of freedom as follows:

- lateral translation of axles (4) x_1, x_2, x_3, x_4
- sideframe lateral translation (2) x_6, x_8
- sideframe rotation over a vertical axle (2) x_5, x_7
- bolster rotation over vertical axle (2) x_9, x_{10}
- carbody rotation over vertical axle (yaw) x_{11}
- carbody lateral translation x_{12}

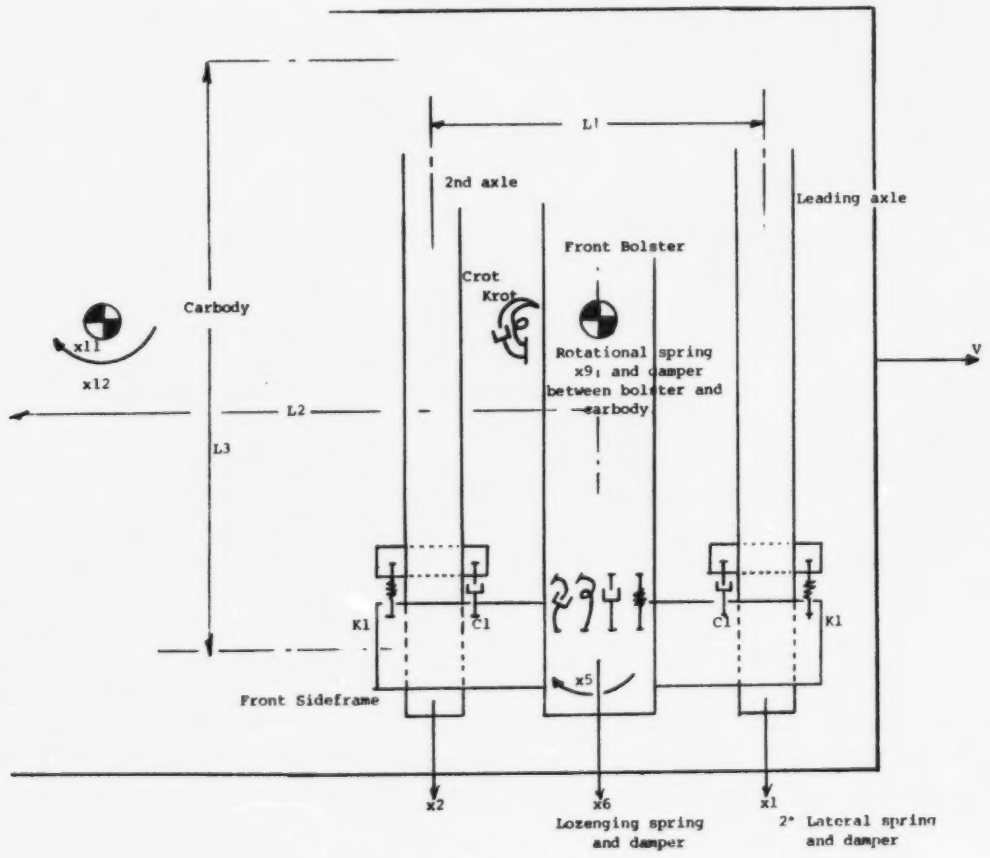

Figure B.7 Schematic of lateral vehicle dynamics model (only front half shown, rear half is identical to front half)

Model inputs include vehicle parameters, track parameters and operating speed. A list of the vehicle parameters is given below:

L_1 = distance between wheels

L_2 = distance between bolsters

M_{ax} = mass of two wheels, axle, bearings, etc., and 1/3 spring

M_{sf} = mass of two sideframes, brakes supports and brakeshoes

M_{bod} = mass of carbody

J_{sf} = rotational inertia of two sideframes

J_{bolst} = rotational inertia of bolster

K_{body} = rotational inertia of carbody

K_{1L}, K_{2L} = primary, secondary lateral stiffnesses doubled

K_{loz} = lozenging stiffness

K_{rot} = rotational stiffness about bolster

K_f, F_d = dry friction parameters

C_{1L}, C_{2L} = primary, secondary damping coefficients doubled

c_{loz} = lozenging damping coefficient

C_{rot} = rotational damping coefficient about bolster

These parameters can be set up to represent a number of railway vehicles. Below are the parameters for a 100-ton car:

L_1	= 1.8 m	K_{2L}	= 6.8 E6 N/m per truck
L_2	= 11.0 m	K_{loz}	= 1 E7 N/m per truck
M_{ax}	= 1,425 kg	K_{rot}	= 1 E7 N/rad
M_{sf}	= 1,460 kg	K_f	= 1 E7 N/m
M_{bod}	= 11,000 kg	F_d	= 1.5 E4
J_{sf}	= 900 Nm^2	C_{1L}	= 6.2 E4 Ns/m
J_{bolst}	= 2,663 Nm^2	C_{2L}	= 3.7 E5 Ns/m
J_{body}	= 18,000,000 Nm^2	C_{loz}	= 1.13 E4 Ns/m per truck
K_{1L}	= 6.8 E7 N/m	C_{rot}	= 40,000 Ns/rad

Track input can be actual alignment errors as recorded by a track geometry car. Currently, brush chart data such as that shown in Figure B.8 are digitized for use as track input.

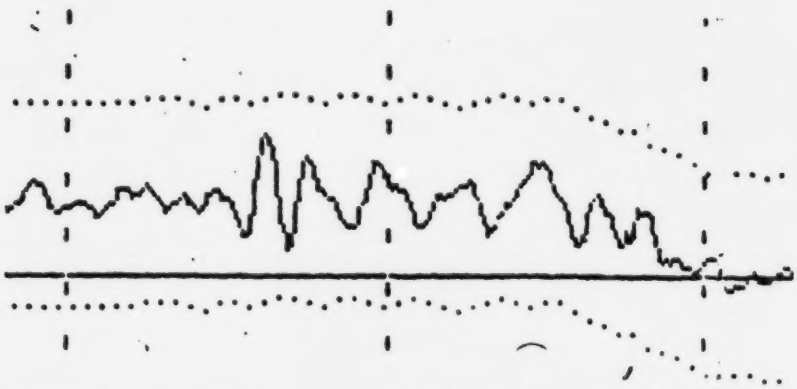

Figure B.8 Sample of brush chart data on alignment error

Figure B.9 is a sample of the model output showing the dynamic variation of the lateral wheel force. Simulation runs can be made for a range of vehicle speeds to estimate the effect of speed on the dynamic lateral wheel force in curved track. This figure is an example result for a 100-ton car.

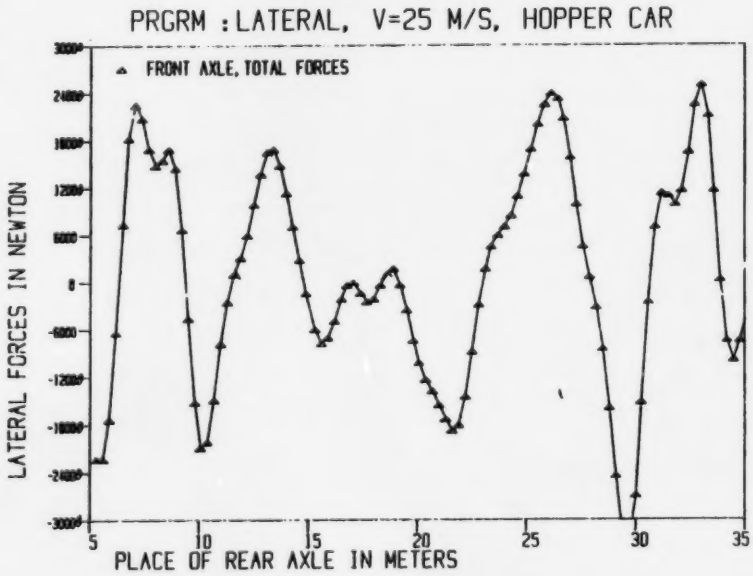

Figure B.9 Sample lateral dynamic vehicle model output

Other vehicle options, such as energy dissipation in the vehicle suspension (as a component of train resistance) can also be made available if required.

APPENDIX C

TRACK DYNAMIC MODEL

C.1 DESCRIPTION

This track dynamic model provides an estimation of the distribution of the dynamic wheel loads by various wheels of a railway vehicle onto the track structure and support components. These data are necessary for accurate evaluation of the effects of different types of traffic on the deterioration of track components and geometry.

The dynamic wheel loads transmitted from a railway vehicle travelling at a given speed over a track with a given level of roughness can be estimated by computer simulations using the vehicle dynamic models developed concurrently in this year's program (see detailed description in Appendix B). These loads are different for each wheel and vary as the vehicle moves along the track. The track dynamic model calculates the different stresses and deformations of the track under each wheel. Details of the calculations are given by Raymond.[1] These data facilitate an analysis of track differential settlement and its consequential effect on track geometry error development.

The model is written in FORTRAN and can be run on an IBM personal computer. Further improvements may be made in the future to link it with the vehicle dynamic models to provide a complete estimate of the stress profile of a track section under a moving vehicle.

C.2 INPUT DATA

The following represent input data on track and vehicle parameters. Values may be changed to simulate various track-loading conditions.

---

1 Raymond, G.P. "North American Track Support Requirements." Transportation Research Board Conference, Washington, D.C., January 14-16, 1985.

TP Tie position (inches): longitudinal coordinate of first crosstie from central control tie (should be a negative number)

TS Tie spacing (inches)

NT Number of ties influencing calculations

E Young's Modulus for rail steel (lb/in^2)

AI Moment of inertia of rail ($in.^4$)

SR Centre-to-centre rail spacing (inches)

NR Number of rails (1 for beam, 2 for conventional track)

U Track modulus (lb/in./in.)

NA Number of axles

MISS Calculation control number; flags - 1, 2, 3, 4:

- 1: calculates rail seat loads, vertical stress and vertical deformation below coordinate (0,0)
- 2: rail seat load and vertical stress (below (0,0))
- 3: rail seat load and deformation (below (0,0))
- 4 or greater: rail seat load only (below (0.0))

WP Wheel load (lbf)

WX Longitudinal coordinate of load (inches) (0 is longitudinal coordinate of control tie)

The following variables are required for stress and deformation calculations:

A Half width of crosstie (inches)

B Half bearing length of crosstie below rail seat (inches)

ANU Equivalent of Poisson's Ratio of soil

Z Depth below coordinate (0,0) at which first value of stress is required (inches)

DZ Depth increment of subsequent stress calculations (inches)

NDZ Number of depth increments for stress calculations

The following variables are required for the settlement calculation:

AH Depth increment for deformation calculations (all calculations start at base of crosstie) (inches)

N Number of depth increments for settlement calculations

NCU Dummy control for future development

AE Equivalent to Young's Modulus for soil layers (values specific to soil layers working downwards from crosstie base) ($lb/in.^2$)

A typical set of input data for North American mainline track is shown in Table C.1.

TABLE C.1

SAMPLE PROGRAM INPUT DATA

TP	-108.0 (in.)	A	4.5 (in.)
TS	18.0 (in.)	B	18.0 (in.)
NT	13	ANV	0.50
E	3.0×13^7 psi	Z	0.0 (in.)
AI	88.1 ($in.^4$)	DZ	32 (in.)
SR	60.0 (in.)	NDZ	1
NR	2	AH	4.0 (in.)
U	3,000 (lb/in./in.)	N	6
NA	4 axles	AE	5,100 ($lb/in.^2$) ballast
WP	32,250 lb		2,500 ($lb/in.^2$) sandy subgrade

OUTPUTS

The model provides data on rail seat load under each wheel. Sample output is shown in Table C.2(a).

TABLE C.2(a)

SAMPLE OUTPUT

```
FOUR  AXLES  ON  132 LB  RAIL
RAIL I=     88.20 TIE SPACING=     18.00 TRACK MODULUS=   3000.00
TRACK MODULUS =   3000.00
NO.OF RAILS= 2     RAIL I=     88.20     RAIL E=   30000000.00
NO. OF TIES= 13    TIE S =     18.00     CO 1ST=       -108.00

          FIRST     RAIL      ;     SECOND    RAIL   ;
        COORDINATE; WHEEL LOAD; COORDINATE; WHEEL LOAD
               .00    32250.00          .00    32250.00
               .00    32250.00          .00    32250.00
               .00    32250.00          .00    32250.00
               .00    32250.00          .00    32250.00

     1         2         3         4
 COORD; SEAT Q; DEFN.; MOMENT; SEAT Q; DEFN.; MOMENT;
-108.00   -424. -.0079 -162056.   -424. -.0079 -162056.
 -90.00   1310.  .0243 -238155.   1310.  .0243 -238155.
 -72.00   4606.  .0853 -288312.   4606.  .0853 -288312.
 -54.00   9762.  .1808 -252724.   9762.  .1808 -252724.
 -36.00  16492.  .3054  -38968.  16492.  .3054  -38968.
 -18.00  23316.  .4318  471932.  23316.  .4318  471932.
    .00  26789.  .4961 1397693.  26789.  .4961 1397693.
  18.00  23316.  .4318  471932.  23316.  .4318  471932.
  36.00  16492.  .3054  -38968.  16492.  .3054  -38968.
  54.00   9762.  .1808 -252724.   9762.  .1808 -252724.
  72.00   4606.  .0853 -288312.   4606.  .0853 -288312.
  90.00   1310.  .0243 -238155.   1310.  .0243 -238155.
 108.00   -424. -.0079 -162056.   -424. -.0079 -162056.
```

1 Distance from loading wheel
2 Rail seat load
3 Elastic track deformation
4 Bending moment

Stress and deformation data from this sample computer run are shown in Tables 3.2(b) and 3.2(c).

TABLE 3.2(b)

SAMPLE OUTPUT

```
     RAIL SPACING =      60.0
     LOAD OF CENTRE CROSSTIE RAILSEATS  =   26788.6   26788.6
RAILSEAT LOAD OF CROSSTIE  1 FROM CENTRE =   23315.6   23315.6
RAILSEAT LOAD OF CROSSTIE  2 FROM CENTRE =   16491.9   16491.9
RAILSEAT LOAD OF CROSSTIE  3 FROM CENTRE =    9762.3    9762.3

     DEFORMATION TIE BASE TO DEPTH - ANU=     .5000

   DEF.[1]        B          D[2]          L     SPACING          E
  .01892    9.00000    4.00000   36.00000   18.00000        5100.
  .04588    9.00000    8.00000   36.00000   18.00000        5100.
  .06821    9.00000   12.00000   36.00000   18.00000        5100.
  .10711    9.00000   16.00000   36.00000   18.00000        2550.
  .14226    9.00000   20.00000   36.00000   18.00000        2550.
  .20559    9.00000   24.00000   36.00000   18.00000        1275.
```

1 Elastic deformation
2 Corresponding depth

TABLE 3.2(c)

SAMPLE OUTPUT

```
14    =NO. AREAS
  .50 =NU
 4.50 =0.5 WIDTH
18.00 =0.5 LENGTH
  .00 =DEPTH 0
32.00 =DZ
 1    =NO. OF DEPTH INCREMENTS

 NU       X        Y        Q        X        Y        Q
  .50   -54.00      .00   9762.25   -54.00    60.00   9762.25
        -36.00      .00  16491.93   -36.00    60.00  16491.93
        -18.00      .00  23315.63   -18.00    60.00  23315.63
          .00       .00  26788.60      .00    60.00  26788.60
        18.00       .00  23315.63    18.00    60.00  23315.63
        36.00       .00  16491.93    36.00    60.00  16491.93
        54.00       .00   9762.25    54.00    60.00   9762.25

 DEPTH  SIG(X)[1]  SIG(Y)  SIG(Z)  SIG(XY)[2]  SIG(YZ)  SIG(ZX)
   .00    82.68    82.68   82.68       .00       .00      .00
 32.00     6.65     5.38   22.42       .00      2.00      .00
```

1 Compressive stress
2 Shear stress

APPENDIX D

RAIL JOINT MAINTENANCE MODEL

4.1 THEORY

Tamping and trowelling at rail joints are major maintenance expenses on BJR track. The cyclic impact loading of the wheel tread as it contacts the dipped geometry of rail joints causes joint settlement, thus requiring frequent tamping and trowelling maintenance measures.

The rail joint maintenance model simulates the dynamic loading at rail joints and predicts subsequent track settlement. A flowchart of the model is shown in Figure D.1.

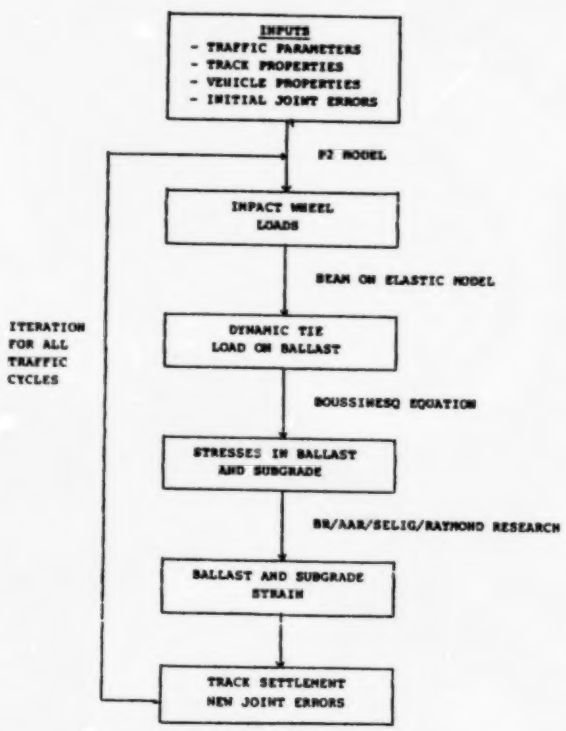

Figure D.1 Flowchart of rail joint maintenance model

The low-frequency dynamic loading at rail joints is estimated using the P_2 formula developed by British Rail for wheel impact loads at rail joints. The formula is shown below.[1]

$$P_2 = P_{ss} + (1-\pi CDR^2 * \frac{M_u}{M_u+M_2}) * 2 \alpha V * 17.6 * \sqrt{K_r * M_u} \sqrt{\frac{M_u}{M_u+M_2}}$$

where:

P_2 = maximum low frequency impact load (N) (lb)
P_{ss} = steady-state wheel load (N) (lb)
CDR = critical damping ratio
M_2 = track mass (kg) (lb-sec^2/in)
M_u = unsprung mass of vehicle (kg) (lb-sec^2/in)
V = vehicle velocity (N/m) (lb/in)
K_r = track stiffness (N/m) (lb/in)
α = track irregularity dip angle (rad)

$$M_2 = (3/2 \ (\frac{MR}{3} + MT) * \frac{1}{12 \times 12 \times 32.2} + MB) * \frac{KRO}{2U}$$

where:

MR = mass of rail (lb/yd)
MT = tie weight (lb/ft)
MB = mass of ballast (lb-sec^2/in)
KRO = track stiffness unloaded (lb/in)
U = track modulus (lb/in/in)

KRO = $2 [(4EI^{.25} \ U^{.25}]$
E = Young's Modulus, I moment of inertia track
KR = KRO $\sqrt{P_2/20,000}$

---

1 D.R. Ahlbeck. "An Investigation of Impact Loads due to Wheel Flats and Rail Joints." ASME 80-WA/RT-1.

The beam on elastic foundation model is used to estimate tie reaction under the wheel load on the ballast. The model and tie reaction formulae are shown in Figure D.2

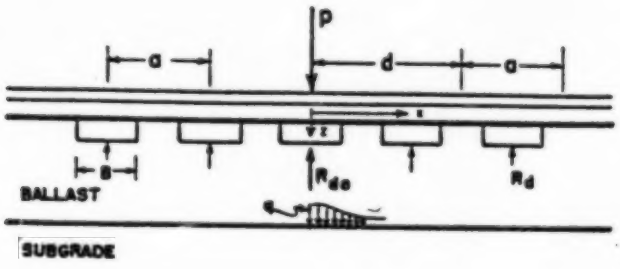

$$R_{d_o}/P = 1 - e^{-\lambda a/2} \cos(\lambda a/2)$$

where: λ = $(U/4EI)^{\frac{1}{4}}$

U = track modulus,

EI = rail stiffness,

a = tie spacing, and

R_{d_o} = tie reaction immediately below the applied load P.

$$\frac{Rd}{P} = \frac{e^{-\lambda d}}{2}\left[\cos\lambda d(1-e^{-\lambda a}\cos\lambda a)+e^{-\lambda a}\sin\lambda a.\sin\lambda d\right]$$

where: d = distance from applied load, P, to nearest mid-space adjacent to the tie under evaluation, and

R_d = the reaction of the tie located d+a/2 away from the applied load

Source: D. Leshchinsky, J. Choros, A.J. Reinschmidt. "Effect of Heavier Axle Loads on Track Substructure Performance." Heavy Haul Conference, 1982

Figure D.2 Beam on elastic foundation

This reaction creates stresses in the ballast and subballast layers. The stress level varies with depth and distance along the track from the tie bearing load as shown in Figure D.3.

Repeated applications of stress cause the ballast to plastically deform. The relationship between the cumulative plastic strain and load cycle at various stress levels is shown in Figure D.4.

From the cumulative plastic strain, the corresponding increase in track settlement can be determined.

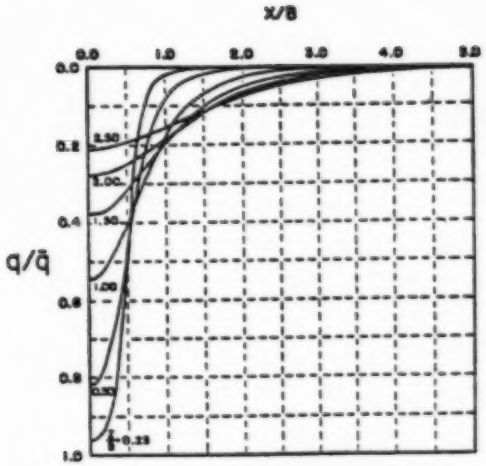

Source: D. Leshchinsky, J. Choros, A.J. Reinschmidt. "Effect of Heavier Axle Loads on Track Substructure Performance." Heavy Haul Conference, 1982

Figure D.3 Non-dimensional presentation of the vertical stress distribution, q, at various depths, z, along the track, x

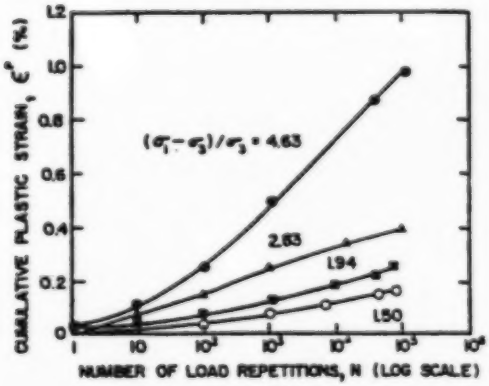

Source: E.T. Selig, J.A. Alva-Hurtado. "Predicting Effects of Repeated Wheel Loading on Track Settlement." Heavy Haul Conference, 1982

Figure D.4 Influence of number of load applications and magnitude of deviator stress on permanent deformation (ref. Barksdale)

D.2 Input/Output

The track input parameters include:

U = track modulus (lb/in/in)
MR = rail weight (lb/yd)
MT = tie weight (lb/ft)
A = tie spacing (in.)
W = tie width (in.)
L = tie length (in.)
II = rail moment of inertia (in^4)
CDR = contact damping ratio
ZB = ballast depth
D = joint dip angle
x = rail joint depth

The vehicle output parameters include:

P_o = static wheel load (lb)
P_{ss} = steady-state wheel load (lb)
M_u = vehicle unsprung mass ($lb\text{-}sec^2/in.$)
V = vehicle speed (mph)
MGT = million gross ton/year

These data must be provided for each of the categories in the traffic mix.

B.5 Output

An example output for rail joint settlement on CN's Kingston Subdivision where thirteen categories of traffic operate is shown in Figure D.5. The impact force and stresses in ballast and subgrade are given for each traffic category. Estimates of plastic strain in ballast and the resulting track settlement are provided for each monthly interval.

```
**********************************************************************************
*                                                                                *
*                          K I N G S T O N   S U B                               *
*                                                                                *
**********************************************************************************

      VEHICLE  1  P0= 5000.  SPEED = 50.MPH  TONNAGE = 1.930 MGT / YR.
      VEHICLE  2  P0=17500.  SPEED = 50.MPH  TONNAGE = 3.502 MGT / YR.
      VEHICLE  3  P0=26250.  SPEED = 50.MPH  TONNAGE = 2.153 MGT / YR.
      VEHICLE  4  P0=28750.  SPEED = 50.MPH  TONNAGE = 0.714 MGT / YR.
      VEHICLE  5  P0=30750.  SPEED = 50.MPH  TONNAGE = 0.411 MGT / YR.
      VEHICLE  6  P0=32000.  SPEED = 50.MPH  TONNAGE = 1.041 MGT / YR.
      VEHICLE  7  P0=32250.  SPEED = 50.MPH  TONNAGE = 0.126 MGT / YR.
      VEHICLE  8  P0= 5000.  SPEED = 60.MPH  TONNAGE = 0.201 MGT / YR.
      VEHICLE  9  P0=17500.  SPEED = 60.MPH  TONNAGE = 1.513 MGT / YR.
      VEHICLE 10  P0=17500.  SPEED = 80.MPH  TONNAGE = 1.389 MGT / YR.
      VEHICLE 11  P0=32792.  SPEED = 50.MPH  TONNAGE = 0.808 MGT / YR.
      VEHICLE 12  P0=32000.  SPEED = 60.MPH  TONNAGE = 0.177 MGT / YR.
      VEHICLE 13  P0=32000.  SPEED = 80.MPH  TONNAGE = 0.811 MGT / YR.
 KB=0.00150

                  X INITIAL JOINT DEPTH = 0.25000 INCHES.
                  ***************************************

      MONTH 1 SIGC=12.00  ALPHA=0.005236
              VEHICLE  1     P2=  6032.  SB= 3.128  SS= 2.377
              VEHICLE  2     P2= 18875.  SB= 9.786  SS= 7.437
              VEHICLE  3     P2= 27765.  SB=14.395  SS=10.940
              VEHICLE  4     P2= 31432.  SB=16.296  SS=12.385
              VEHICLE  5     P2= 33474.  SB=17.355  SS=13.190
              VEHICLE  6     P2= 34750.  SB=18.017  SS=13.693
              VEHICLE  7     P2= 35005.  SB=18.149  SS=13.793
              VEHICLE  8     P2=  7228.  SB= 3.748  SS= 2.848
              VEHICLE  9     P2= 20389.  SB=10.571  SS= 8.034
              VEHICLE 10     P2= 20002.  SB=10.371  SS= 7.882
              VEHICLE 11     P2= 44135.  SB=22.882  SS=17.391
              VEHICLE 12     P2= 42791.  SB=22.186  SS=16.861
              VEHICLE 13     P2= 46702.  SB=24.214  SS=18.402
 BALLAST STRAIN=0.0019636   SETTLEMENT= 0.2736

      MONTH 2 SIGC=12.00  ALPHA=0.005729
              VEHICLE  1     P2=  6134.  SB= 3.180  SS= 2.417
              VEHICLE  2     P2= 19007.  SB= 9.855  SS= 7.490
              VEHICLE  3     P2= 27909.  SB=14.470  SS=10.997
              VEHICLE  4     P2= 31690.  SB=16.430  SS=12.487
              VEHICLE  5     P2= 33737.  SB=17.491  SS=13.293
              VEHICLE  6     P2= 35015.  SB=18.154  SS=13.797
              VEHICLE  7     P2= 35270.  SB=18.286  SS=13.898
              VEHICLE  8     P2=  7457.  SB= 3.866  SS= 2.938
              VEHICLE  9     P2= 20672.  SB=10.718  SS= 8.146
              VEHICLE 10     P2= 20246.  SB=10.497  SS= 7.978
              VEHICLE 11     P2= 45283.  SB=23.478  SS=17.843
              VEHICLE 12     P2= 43882.  SB=22.751  SS=17.291
              VEHICLE 13     P2= 48225.  SB=25.003  SS=19.002
 BALLAST STRAIN=0.0021663   SETTLEMENT= 0.2760
```

Figure D.5 Sample output

APPENDIX E

TURN-OUT MAINTENANCE MODEL

E.1 INTRODUCTION

E.1.1 Objective

In railway track, turn-outs normally require high maintenance; this maintenance requirement is a significant component of track maintenance cost. Where mixed traffic operates, it is often difficult to estimate the proportion of turn-out damage and cost attributable to each traffic category. This report examines the nature of turn-out maintenance problems and determines the relative damage caused by each traffic category.

E.1.2 Nature of Turn-Out Maintenance Problems

An on-site investigation of turn-out problems was conducted at a track location near Kingston. A CN engineer and a maintenance supervisor assisted with the examination and interpretation. The following are the main observations:

- major damage is caused by straight-through traffic
- frog damage is predominantly in the form of plastic deformation of the nose and wings
- switch point damage is also predominantly plastic deformation at a short distance from the point.

These observations indicate that the major cause of damage is the impact force of the wheel tread as it contacts the dipped geometry of the frog nose and switch point. This force is similar to the P_2 low-frequency impact load occurring at dipped joints. Because the force is speed-dependent, damage is greater in the straight-through direction where train speeds are high.

The slope at a frog nose and switch point (see Figures E.1 and E.2) is designed to protect the points from a direct wheel strike as the vehicle leaves the main rail. As the wheel is forced to climb the incline, a P_2-type impact results. The nose of the frog receives the impact approximately 21" from the half-inch point and the switch point impact loading occurs approximately 18" from the point.

Plastic deformation of frogs and switches is the main result of the repeated impacts, and leads to the usual maintenance requirements of grinding, welding and eventual replacement. Other modes of damage such as surface fatigue cracks are associated with impact loading, but as plastic deformation is the main factor, it is a good proxy for those modes. An analysis based solely on the relationship between wheel impacts is therefore considered a reasonable method for estimating the influence of various types of traffic on frog and switch maintenance.

E.1.3 Method of Analysis

The process of plastic deformation is analogous to fatigue failure in that there is a general threshold level of impact force below which there is no damage, and above which damage will occur with increasing severity. Therefore, in a mixed traffic operation where each traffic category generates a different impact load, the share of the deformation is essentially non-linear, i.e. doubling the wheel impact force causes more than double the damage and certain low impact forces may not contribute to damage at all.

Current knowledge in contact mechanics applicable to wheel/rail contact situations and plastic deformation of rail steel can be employed to quantify the relative damage level associated with each impact force level from each traffic category. These relative damage levels are then multiplied by the number of loading cycles of each traffic category to give their total contribution. The per cent damage attributable to a given traffic category is the ratio of its total contribution to the grand total contribution by all traffic categories.

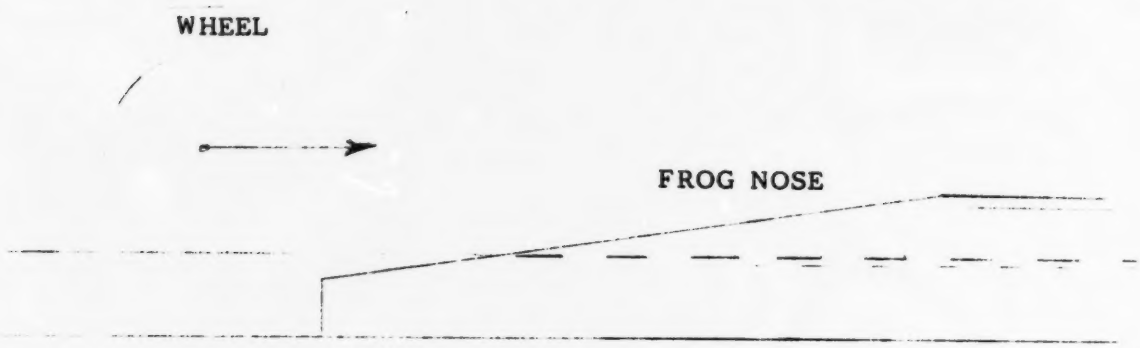

Figure E.1 A wheel approach to a frog nose

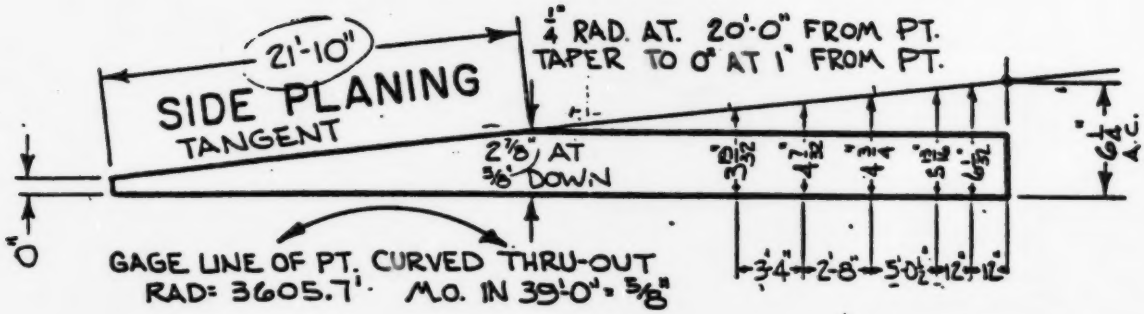

Figure E.2 Point of switch

E.2 THEORY

E.2.1 Impact Model

Impact loading at frog noses and switch points can be estimated by the P_2 impact force model developed for dipped rail joints:[1]

$$P_2 = Pss + (1 - CDR^2 \frac{M2}{Mu+M2}) * \alpha 2\ V(17.6)\ \sqrt{KR*Mu}\ \sqrt{\frac{Mu}{Mu+M2}} \quad (1)$$

where the vehicle parameters are:

- Pss = steady-state axle load (N) (lb)
- Mu = unsprung mass (kg) (lb sec^2/m)
- V = vehicle velocity (m/s) (in/s)
- α = mph x 17.6

and where the track parameters are:

- CDR = critical damping ratio (0.7)
- E = Young's Modulus (lb/in)
- I = rail inertia (in^4)
- U = track modulus (lb/in/in)
- KRO = track stiffness unloaded
  ($KRO = 2 * (4EI)^{.25} * U^{.75}$)
- KR = track stiffness loaded
  (iterative calculation with P_2 starting with:

$$KR = KRO * \sqrt{\frac{Po}{20,000}})$$

---

1 D.R. Ahlbeck. "An Investigation of Impact Loads Due to Wheel Flats and Rail Joints." ASME Publication 80-WA/RT-1.

M2 = track mass:

$$M2 = 3/2 \left[\left(\frac{MR + Mt}{12} \right) * \frac{1}{12x12x32.2} + MB \right] * \frac{KRO}{2U}$$

MR = mass of rail (lb/yd)

MT = tie weight (lb/ft)

MB = mass of ballast (lb-sec^2/in)

α = dip angle at frog or switch (radians)

For frogs, α is the slope angle of the nose at a location 21" from the half-inch point. For a #20 frog, α = 0.01989 radian.

For switches, α is the slope angle of the point at a location 18" from the point. For a #20 switch, α = 0.00244.

Track mass and stiffness are not constant throughout a turn-out section. Longer ties, extra rail sections and ballast at frogs increase track mass at frog locations. The extra rail required at these sites also increases track stiffness. Based on Figure E.3, it is estimated that for a frog:

$$I = 2 * I \text{ stockrail} + I \text{ frog}$$

At the site of the switch points there is no significant change in track mass compared to standard track. Therefore, it is estimated that for a switch:

$$I = I \text{ rail}$$

Figure E.3 Frog nose cross-section

E.2.2 Plastic Deformation Model

E.2.2.1 Stress Analysis

The maximum contact stress generated when a wheel impacts on a frog or switch can be calculated using the Hertzian formula in which the dynamic load and wheel and rail contact geometries determine the stress level. It it given by:

$$P_{max} = \frac{1}{\pi} \left(\frac{3}{2}\right)^{1/3} \left(\frac{G\,\mathcal{E}(1/R)}{(1-\upsilon)}\right)^{2/3} * W^{1/3} \qquad (2)$$

where:
P_{max} = contact stress (psi)
W = dynamic load (lbs)
G = 11.5×10^6 psi
υ = 0.29
$\mathcal{E}(\frac{1}{R})$ = $\frac{1}{Rw} + \frac{1}{Rr} + \frac{1}{R^1w} + \frac{1}{R^1r}$
Rw = longitudinal wheel radius = 18" new, 20" locomotive
Rr = longitudinal rail radius = ∞
R^1w = wheel radius in transverse vertical plane = ∞
R^1r = rail radius in transverse vertical plane
R^1rail = 4" (estimated for frog)
R^1rail = 9" (estimated for switch)

$$\text{Frog } P_{max} = 23{,}452 \left(\frac{1}{18} + \frac{1}{4}\right)^{2/3} * P_2^{1/3}$$

$$\text{Switch } P_{max} = 23{,}452 \left(\frac{1}{18} + \frac{1}{4}\right)^{2/3} * P_2^{1/3}$$

E.2.2.2 Shakedown Limit

Stresses caused by dynamic loading do not always cause plastic deformation. Many forces do not create stresses above the elastic limit of the metal. A major consideration in deformation calculations is not only the yield point of the material, but its effective yield point. Also termed the "shakedown limit," this is the stress level at which plastic deformation will occur.

The shakedown limit of a metal in service is related to metal hardness. The initial hardness increases in a work-hardened manner as cyclic loading occurs. This increase in hardness extends the metal's elastic zone and defines the new yield point and shakedown limit.

Work by Tabor suggests that the yield point of steel can be estimated by:

$$k = \frac{1}{6} \text{ DPH}$$

where Vickers hardness DPH = 1.05 Brinell Hardness Number and the shakedown limit can be estimated by:

$$SL = 4 \times \frac{1}{6} \times 1.05 \text{ BHN} \qquad (3)$$

From CN data on hardness of frogs in new and worn conditions, an average hardness is estimated as:

$$\text{Average BHN Frog} = \left(\frac{300 + 600}{2}\right) = 450$$

and the average shakedown limit is:

$$\text{Average SL Frog} = 4 \times \frac{1}{6} (1.05)\ (450) = 315.0 \text{ kpsi}$$

Similarly, for switches:

$$\text{Average BHN Switch} = \left(\frac{300 + 360}{2}\right) = 330.0$$

$$\text{Average SL Switchpoint} = 4 \times \frac{1}{6} \times (1.05) \times (330.0) = 231.00 \text{ kpsi}$$

E.2.2.3 Plastic Deformation

Prior to shakedown (e.g. first cycle), plastic deformation may occur only if maximum contact stress (P_{max}) exceeds the yield point times a restraining factor (about 1.7 for steel).

After shakedown has been established, plastic deformation may occur only if maximum contact stress (P_{max}) exceeds the shakedown limit (effective yield point).

The relationship between stress and strain in the plastic deformation range for metal is given by:[2]

$$\sigma = \overset{\text{constant n}}{\varepsilon} \quad \text{or} \quad \varepsilon = \sigma^{k}$$

where: n = work-hardening exponent

k = 1/n

---

2 "Mechanical Properties of Materials." Marks' Standard Handbook for Mechanical Engineers. 8th edition, pp.5.4-5.5.

This relationship and the theory of shakedown can be adapted to establish a formula for the estimation of plastic deformation levels associated with an impact wheel load. For practical consideration, it is noted that there is a range of hardness for each frog and switch. The variation is due to the non-uniformity of the metallurgy and the work-hardening pattern. In addition, frogs and switches are generally softer when new and become harder with work-hardening in service. Within a given range of hardness, there is a corresponding range of shakedown limits. The shakedown limit cannot be positively defined for the calculation of plastic deformation. It is probably correct to assume that plastic deformation will more likely occur if the maximum applying contact stress is greater than the shakedown limit associated with the mean hardness value and vice versa.

Therefore, it is proposed that the amount of plastic deformation caused by a wheel impact force associated with a maximum contact stress, P_{max}, be estimated by:

$$p = \text{constant} * y * (P_{max} - P_{yield})^{k} \qquad (4)$$

where: k = inverse of the work-hardening exponent

P_{yield} = yield point

y = probability of causing plastic deformation.

"y" is given by:

$$y = \frac{1}{2} [\, 1 + \tanh x]$$

where: $x = (P_{max} - SL)/SL$

Figure E.4 is a graphical representation of y. It gives a 0.5 probability of plastic deformation if the impact causes contact stress equal to the mean shakedown limit (based on mean hardness). For contact stress greater than the maximum shakedown limit, the probability is virtually unity (1.0).

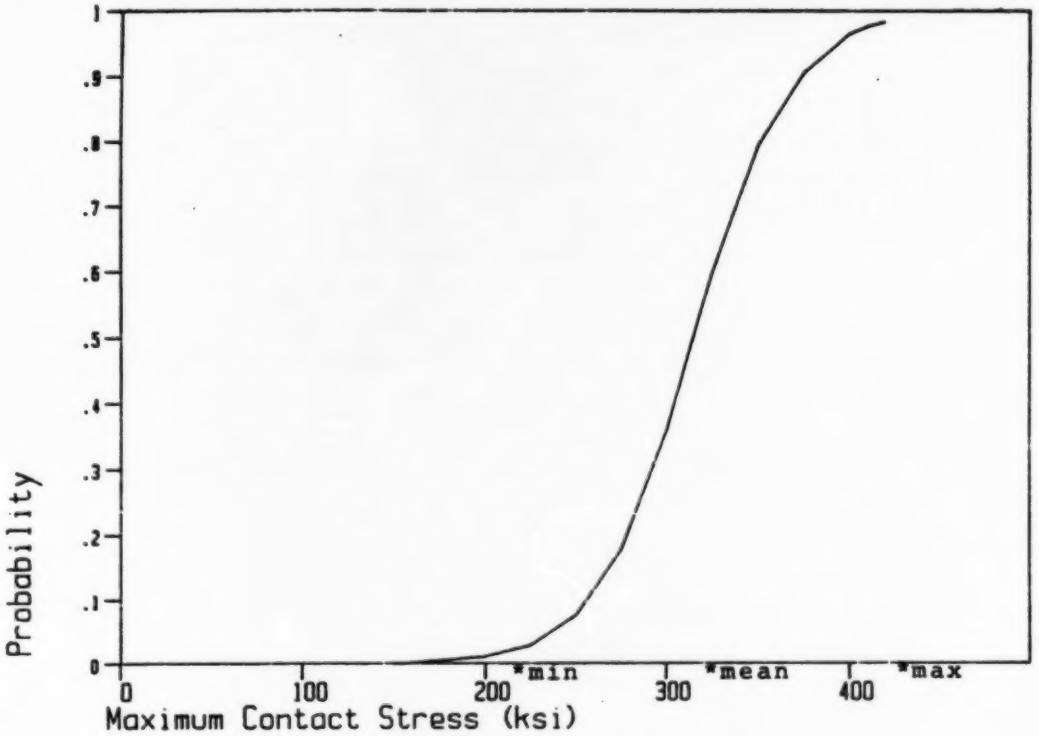

* minimum shakedown limit 210,000 psi corresponds to minimum Brinell Hardness Number 300

* mean shakedown limit at 315,000 psi, 450 BHN

* maximum shakedown limit 420,000 psi, 600 BHN

Figure E.4 Deformation versus stress level

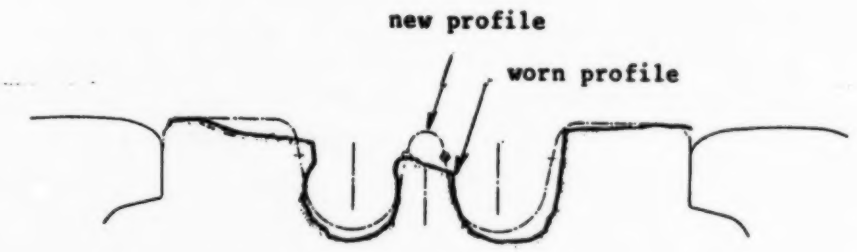

Figure E.5 Plastic deformation of frog nose

For contact stress less than the minimum shakedown limit, the chance is practically zero. It is not certain what k should be for frogs and switches. For mild steel it is 4. Without better information, 4 is assumed to be the value for frogs and switches also. (Please refer to a sensitivity analysis on the effect of uncertainty of this "k" value included in Section E.5 of this appendix.)

From equation (4), damage factor DF_i, the total plastic deformation contributed by a traffic category, i, can be estimated as:

$$DF_i = p_i \times y_i \times N_i \qquad (5)$$

where N_i is the number of wheel loading cycles in category i.

The per cent share of the total frog or switch damage is therefore:

$$R_i = 100 \times \frac{DF_i}{\sum_{j=1}^{M} DF_j} \qquad (6)$$

where: M = number of traffic categories.

3. COMPUTER MODEL

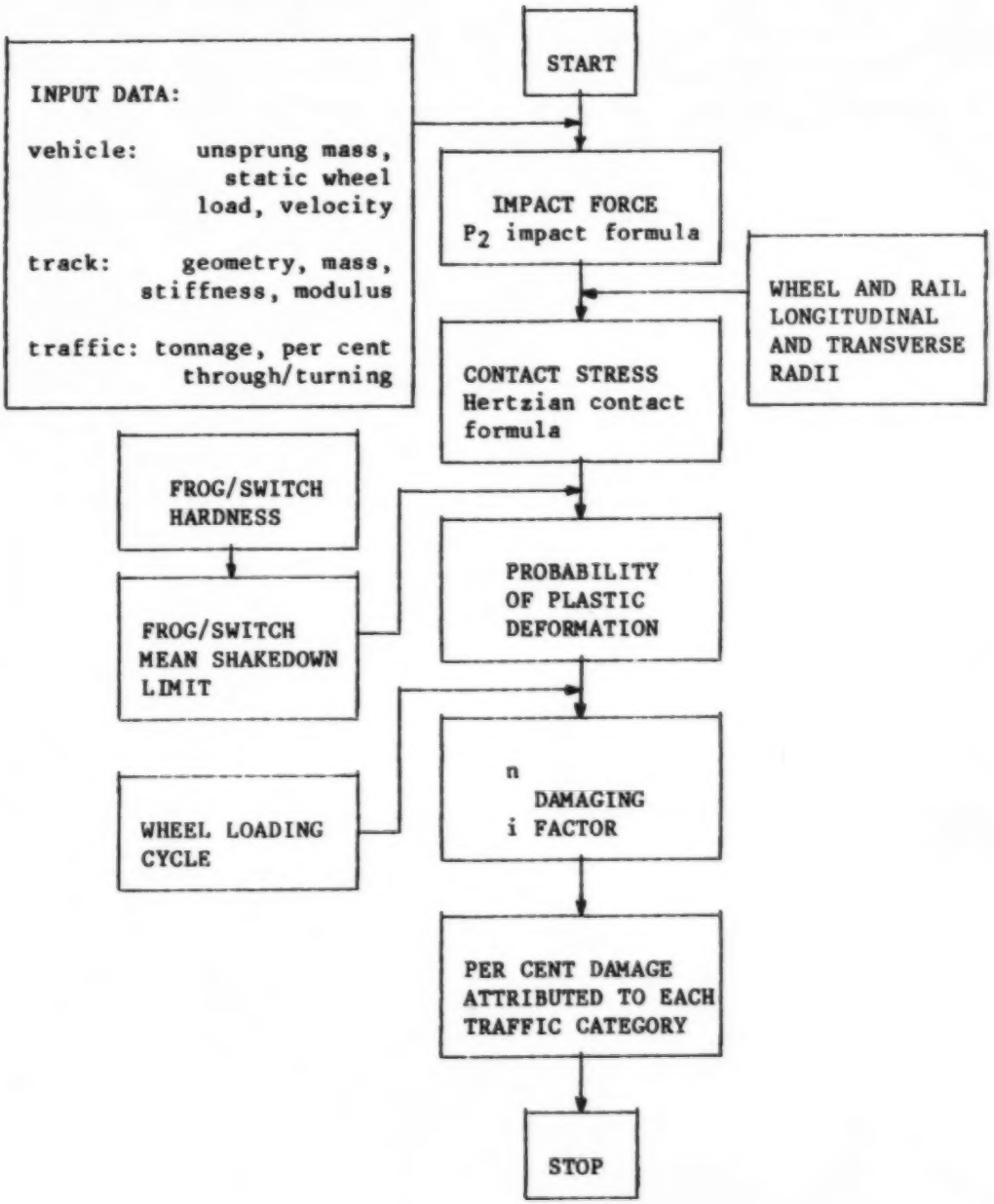

Figure E.6 Flow diagram

APPENDIX F

TIE LIFE MODEL

F.1 DESCRIPTION

The tie life model predicts the number of tie replacements per year based on the annual tonnage of a mixed traffic operation. It can be used to forecast future tie renewal requirements for a given track subject to a given level of traffic. The model also provides a breakdown of total tie replacement into per-traffic and per-track categories. These outputs render the model useful for cost-sharing and resource-allocation analyses in a railway system with a mix of traffic and a mix of track geometry (tangent, curves, etc.). Figure F.1 is a flow diagram which outlines the calculation procedure in this model. "VDM" represents a set of vehicle dynamic models which give the dynamic vertical and lateral wheel forces exerted on the track by a railway vehicle. These models take into account the nominal vehicle weight, vehicle speed and track roughness. This allows for the differentiation of tie damage contribution by tonnage from a heavy/light or fast/slow railway vehicle over smooth or rough track.

The model is set up on the Lotus 1-2-3. A complete listing of the input and output data is shown in Figures F.2 and F.3.

F.2 SAMPLE APPLICATION

To illustrate its application, the model is used to predict the annual tie replacement on CP's Cascade subdivision. Table F.1 describes the track and traffic characteristics over this subdivision. There was a progressive change from BJR to CWR over the years in relation to the progressive increase in the percentage of 100-ton cars (heaviest axle load). These trends are illustrates in Figures F.4 and F.5. The annual tonnage also increased gradually from 20 MGT in 1965 to 45 MGT in 1982. This trend is shown in Figure F.6.

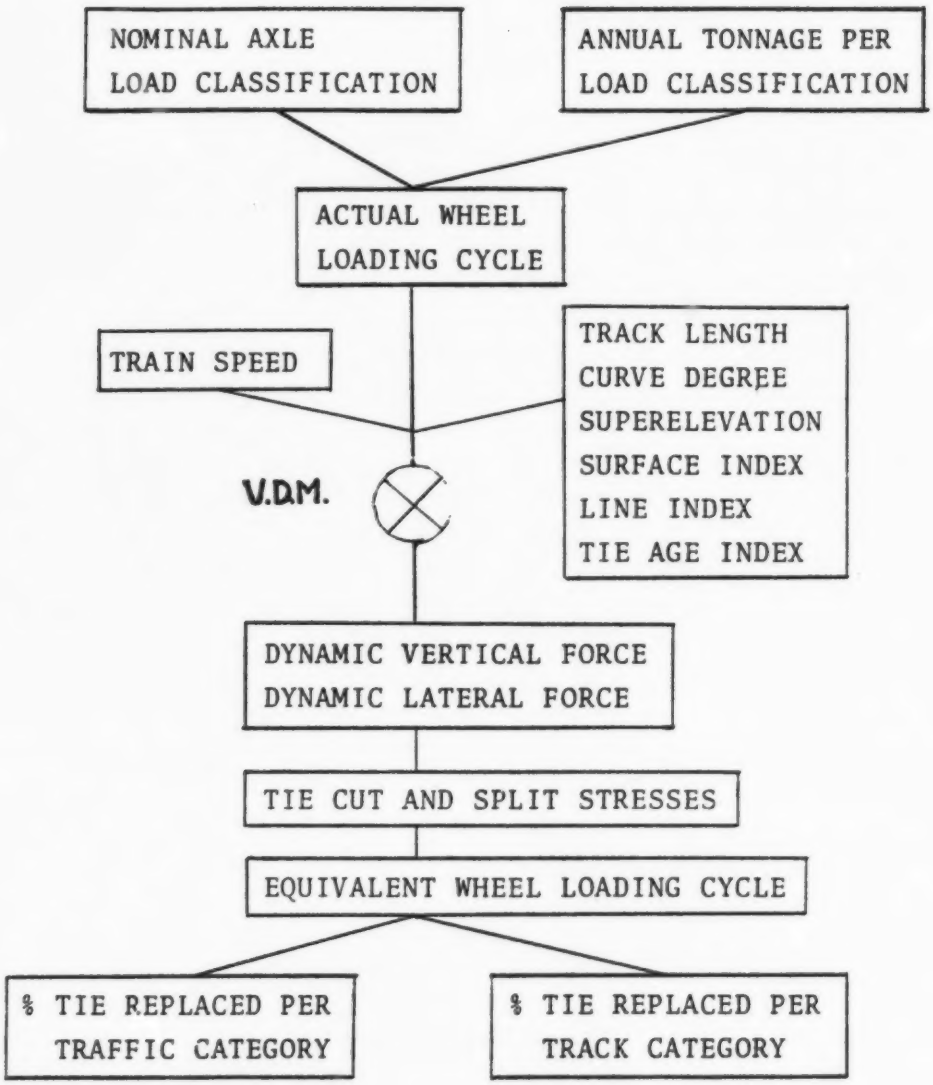

Figure F.1 Tie life calculation flow chart

nom.axle load US ton	annual tonnage US ton	average speed mph	track length mile	degree of curve
8.00	10728000.00	45.00	78.00	0.00
20.00	11622000.00	45.00	78.00	0.00
33.00	22350000.00	45.00	78.00	0.00
8.00	10728000.00	40.00	25.00	2.00
20.00	11622000.00	40.00	25.00	2.00
33.00	22350000.00	40.00	25.00	2.00
8.00	10728000.00	35.00	37.00	5.00
20.00	11622000.00	35.00	37.00	5.00
33.00	22350000.00	35.00	37.00	5.00
8.00	10728000.00	30.00	25.00	8.00
20.00	11622000.00	30.00	25.00	8.00
33.00	22350000.00	30.00	25.00	8.00

superelevation in	surface index	alignment index	tie ase index
0.00	1.02	1.02	1.50
0.00	1.02	1.02	1.50
0.00	1.02	1.02	1.50
	1.02	1.02	1.50
	1.02	1.02	1.50
1.00	1.02	1.02	1.50
1.00	1.02	1.02	1.50
1.00	1.02	1.02	1.50
2.00	1.07	1.07	1.50
2.00	1.07	1.07	1.50
2.00	1.07	1.07	1.50
	1.07	1.07	1.50
	1.07	1.07	1.50
2.50	1.07	1.07	1.50
2.50	1.07	1.07	1.50
2.50	1.07	1.07	1.50

Figure F.2 Input

actual cycle	static V load lb	steady V load lb	dynamic V load lb	steady L load lb	dynamic L load lb	dynamic V rail seat load lb	dynamic L rail seat load lb
1341000.00	8000.00	8000.00	8923.96	373.65	868.23	2677.19	260.47
581100.00	20000.00	20000.00	22309.90	688.48	1924.93	6692.97	577.48
677272.73	33000.00	33000.00	36811.33	961.51	3001.65	11043.40	900.50
1341000.00	8000.00	8423.50	9323.61	2345.80	2743.07	2797.08	822.92
581100.00	20000.00	21058.75	23309.02	4322.31	5315.50	6992.71	1594.65
677272.73	33000.00	34746.94	38459.88	6036.40	7675.16	11537.97	2302.55
1341000.00	8000.00	8764.75	9664.35	3644.06	3969.15	2899.31	1190.75
581100.00	20000.00	21911.87	24160.88	6714.46	7527.20	7248.26	2258.16
677272.73	33000.00	36154.59	39865.45	9377.20	10718.21	11959.63	3215.46
1341000.00	8000.00	8831.21	9649.95	4612.77	4856.83	2894.99	1457.05
581100.00	20000.00	22078.03	24124.88	8499.40	9109.54	7237.47	2732.86
677272.73	33000.00	36428.75	39806.06	11869.98	12876.71	11941.82	3863.01

cut stress psi	split stress psi	equiv.cut cycle	equiv.split cycle	'cut cycl.mile	split cycl.mile
31.39	220.02	1349234.17	1350086.38	105240265.59	105306737.74
51.94	533.24	1244723.36	2207413.99	97088422.14	172178291.14
84.03	867.92	2985065.21	5342265.51	232835086.68	416696709.92
40.32	355.45	1964302.75	2772318.66	49107568.72	69307966.57
85.99	783.14	2651290.03	3928772.76	66282250.87	98219319.10
131.37	1217.26	5834872.29	8873250.29	145871807.17	221831257.25
52.60	445.45	2927041.01	3889282.06	108300517.50	143903436.27
108.50	949.76	3757739.34	5247032.28	139036355.57	194140194.18
162.69	1450.70	8041434.69	11544532.78	297533083.37	427147712.92
61.10	505.91	3664480.09	4707371.59	91612002.24	117684289.75
123.64	1057.34	4570881.77	6163360.78	114272044.25	154084019.39
183.33	1597.28	9618655.95	13337612.12	240466398.87	333440303.12

Figure F.3 Output

Grand total cut cycle mile	Grand total split cycle.mile	% cut replace per traffic cat.	% split replace per traffic cat.	% cut replace per track cat	% split replace per track cat
1687645802.96	2453940237.35	20.99	17.78	25.79	28.29
		24.69	25.21		
		54.32	57.02		
				15.48	15.87
				32.29	31.18
				26.45	24.66

total cut ton stdized @ 8T	total split ton stdized @ 8T	total tonnage stdized @ 8T	mech tie loss per MGT	total mech tie loss per yr	other tie loss per yr
337529160.59	490788047.47	430112738.43	95.25	40968.24	3226.25

YEAR :	1982.00
MECH TIE LOSS :	40968.24
OTHER TIE LOSS :	3226.25
TOTAL TIE LOSS :	44194.49

Figure F.3 (Cont'd) Output

TABLE F.1

CP TIE REPLACEMENT DATA -- CASCADE SUBDIVISION[1]

	1965	1966	1967	1968	1969	1970	1971	1972	1973	1974	1975	1976	1977	1978	1979	1980	1981	1982
Ties (000)[2]	33	25.8	31	45	1.2	2.0	32.4	24	20.9	68.6	8.1	15.2	33.6	29.5	11.5	85.9	51.7	59.4
MGT	20.4	22.3	22.9	23.8	23.5	26.9	30.7	33.1	36.8(36)		35.8	34.3	37.5	41.3	41.4	40.5	45.8	44.7
Per Cent MGT:																		
per cent 100-ton[3]	0	0	0	2	5	9	14	19	24	29	33	36	39	42	45	47	48.5	50
per cent empty[4]	24	24	24	24	24	24	24	24	24	24	24	24	24	24	24	24	24	24
per cent general[5]	76	76	76	74	71	67	62	57	52	47	43	40	37	34	31	29	27.5	26
Per cent CWR	0	0	0	0	0	3	6	10	16	22	28	35	42.5	50	60	70	79.5	89
Per cent BJR	100	100	100	100	100	97	94	90	84	78	72	65	67.5	50	40	30	20.5	11

	Distance (miles)	No. of Spikes	Plate	Speed (mph)	Super-elevation	Deficiency
Tangent	78	2	14"	45	0	0
Up yo 3° curve	25	3	14"	40	1"	(-1")
3° to 6° curve	37	5	18"	35	2"	(-1.8")
Greater than 6° curve	25	5	18"	30"	2.5"	(-2")

1 From R. McIlveen, Financial Planning Department, CP
2 Total: 578,800 ties (total ties in 165 mile section: approx. 500,000)
3 33-ton axle load
4 8-ton axle load
5 20-ton axle load

The model is applied for the track/traffic and tonnage conditions in each year to arrive at a predicted number of tie replacements. Overall tie age on the entire track section is assumed constant, since from 1965 to 1985 virtually all ties have been replaced (578,800 ties replaced versus about 500,000 ties in 165 miles of track). The predicted data are plotted against the actual ones in Figure F.7. The straight line shown is a line of best fit through the actual data. It serves as a general guide on one tie replacement trend in this subdivision from 1965 to 1982 (seventeen years). As shown, the prediction agrees quite well with the general trend. It should be noted that actual tie replacement on a yearly basis is not stable but is greatly influenced by management decision. Consequently, prediction should be compared against the general trend line. The predicted tie replacement curve also responds to the short cycle fluctuation in tonnage. This makes it more useful than a simple regression of past tie replacement data (as is the case for

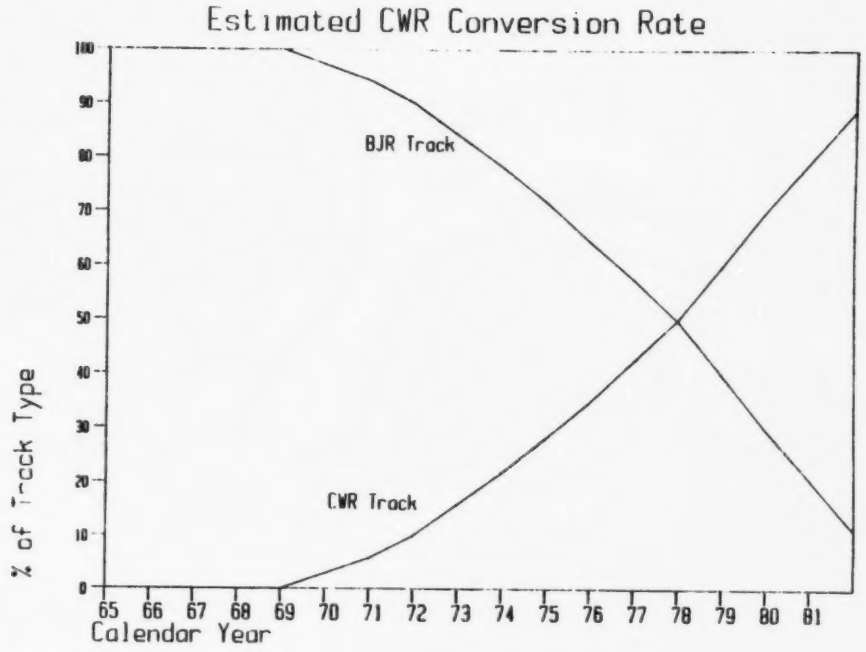

Figure F.4 Estimated CWR conversion rate

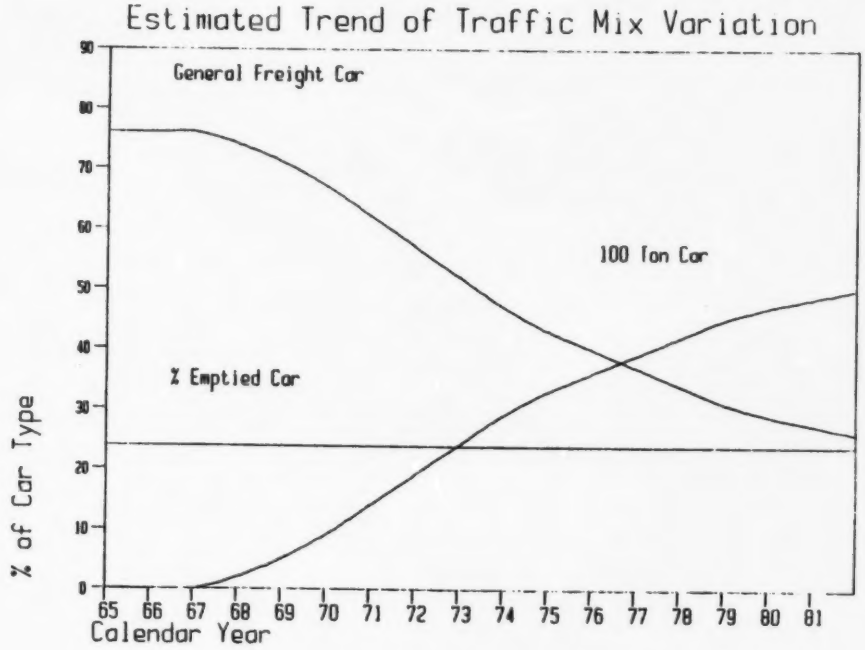

Figure F.5 Estimated trend of traffic mix variation

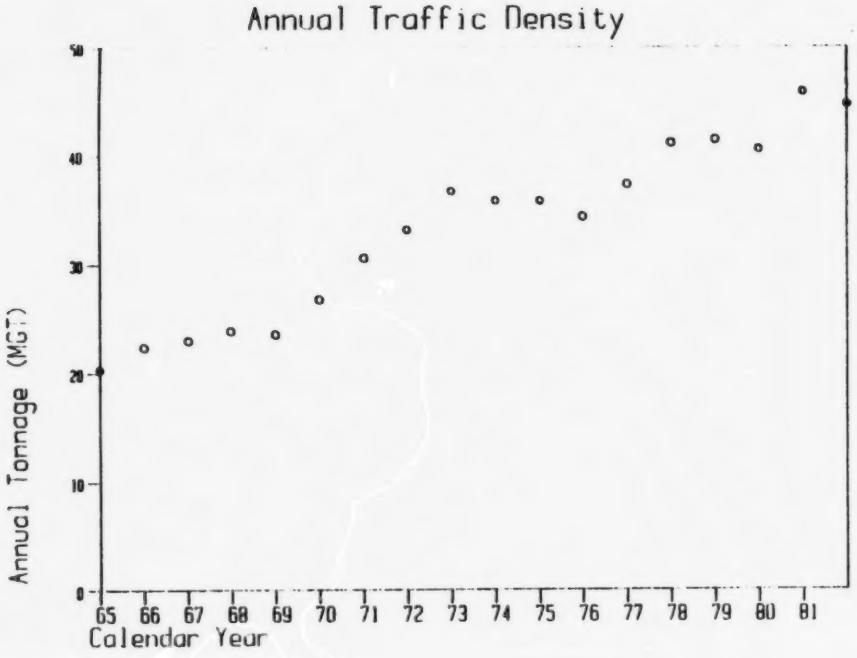

Figure F.6 Annual traffic density

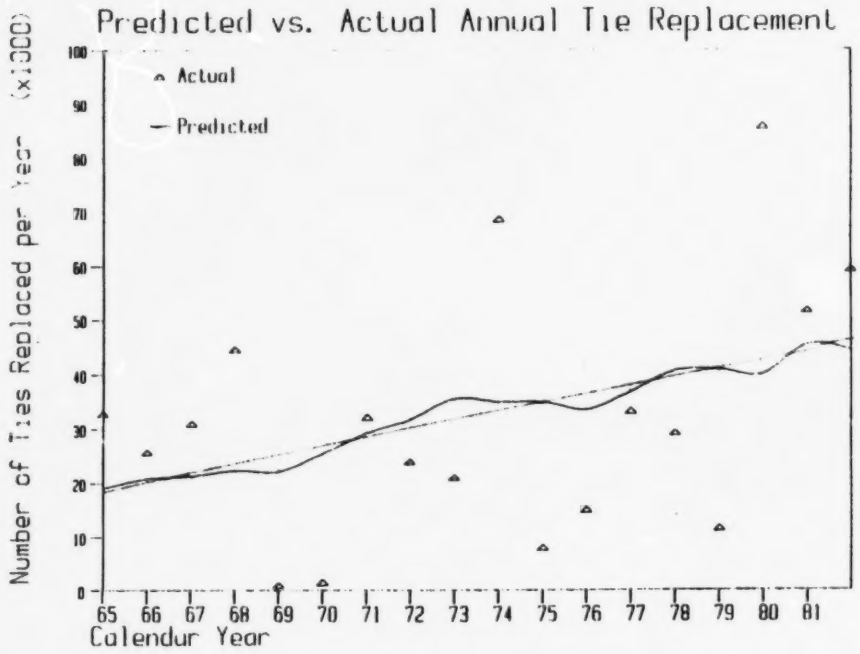

Figure F.7 Annual tie replacement

some existing tie replacement models). It can also be seen from this figure that the small rate of increase in percentage of 100-ton cars in later years (1978 to 1980) is balanced out by the sharp increase in the percentage of CWR due to the track upgrading program.